Smooth Muscle Tumors of the Uterus at MRI: Focus on Leiomyomas and FIGO Classification

Wendy Tu, MD, FRCPC • Motoyo Yano, MD, PhD • Nicola Schieda, MD, FRCPC • Satheesh Krishna, MD
Longwen Chen, MD, PhD • Ravi V. Gottumukkala, MD • Raquel Alencar, MD, PhD

Author affiliations, funding, and conflicts of interest are listed at the end of this article.
See the invited commentary by Fennessy and Gargiulo in this issue.

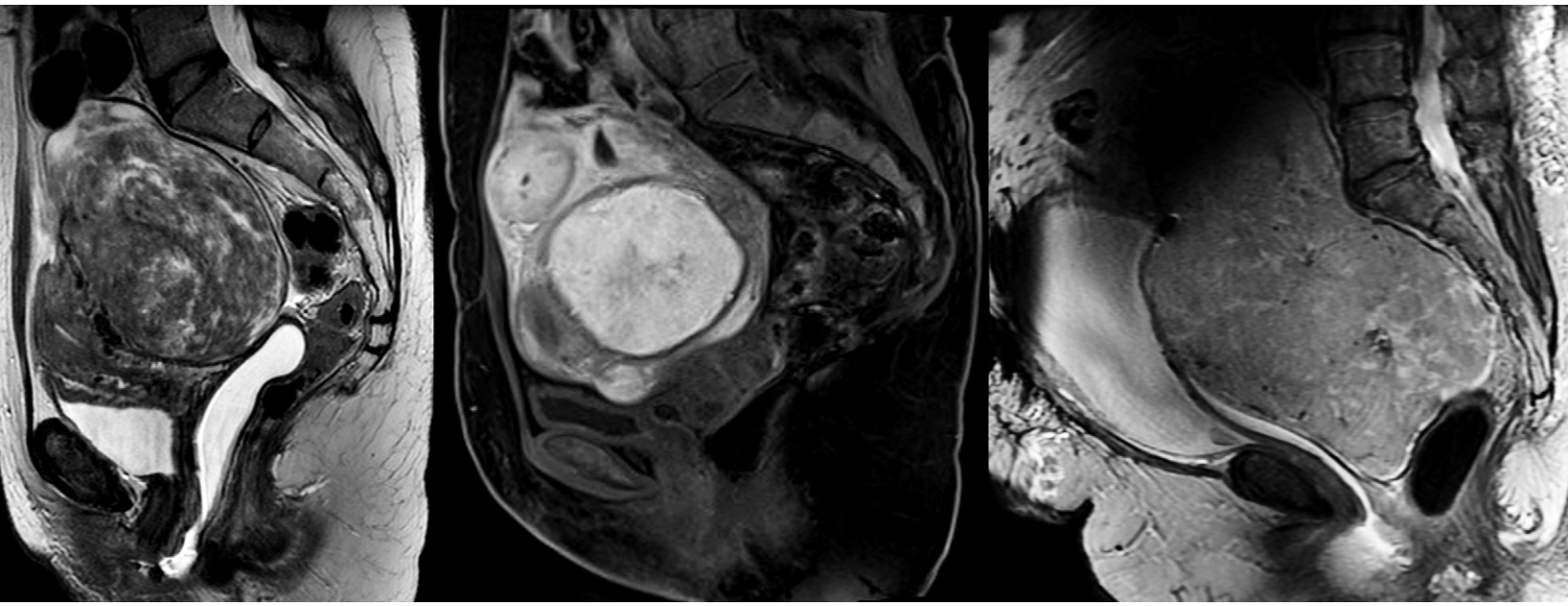

Leiomyomas are smooth muscle tumors of the uterus and are the most common uterine neoplasm. Although leiomyomas are usually asymptomatic, they can manifest with symptoms such as pain or uterine bleeding. Leiomyomas are classified on the basis of their anatomic location and morphology. Localization of leiomyomas relative to the endometrium, myometrium, and uterine serosa with use of the International Federation of Gynecology and Obstetrics (FIGO) classification system is helpful for guiding management in symptomatic patients. The FIGO system is a practical and universally accepted approach for classifying leiomyomas to guide radiologists and clinicians in deciding management. The MRI appearance of conventional leiomyomas is related to their tissue contents of smooth muscle and fibrous tissue and is well established. The MRI features of some leiomyoma subtypes and forms of degeneration also have been described. Other smooth muscle tumors of the uterus recognized in the 2020 World Health Organization classification system include intravenous leiomyomatosis, smooth muscle tumors of uncertain malignant potential, and metastasizing leiomyoma. At the far end of the spectrum are leiomyosarcomas, which are frankly malignant and therefore must be managed accordingly. Although MRI features that suggest a diagnosis of leiomyosarcoma have been proposed, these features overlap with those of some leiomyoma subtypes and degeneration.

Introduction

Uterine leiomyomas, also known as fibroids, are the most common gynecologic and uterine neoplasm (1). At pathologic analysis, they have a low mitotic index (fewer than five mitoses per 10 high-power fields), no cellular necrosis (with the exception of tumor ischemia–induced degeneration), no significant cytologic atypia, no intravascular component, uniformly sized and shaped spindle-shaped cells, and well-circumscribed borders (2).

Uterine leiomyomas are hormonally dependent benign smooth muscle tumors that develop after menarche and typically regress after menopause (1). The lifetime prevalence of leiomyomas exceeds 70% in women (3). The incidence is especially high in African-American patients (two to three times

Invited Commentary

Slide Presentation

Supplemental Material

CME Quiz questions for this article are available through the Online Learning Center.

RadioGraphics 2023; 43(6):e220161
https://doi.org/10.1148/rg.220161

Content Codes: MR, OB

Abbreviations: ADC = apparent diffusion coefficient, FIGO = International Federation of Gynecology and Obstetrics, H-E = hematoxylin and eosin, ROI = region of interest, STUMP = smooth muscle tumor of uncertain malignant potential, T1W = T1 weighted, T2W = T2 weighted, UFE = uterine fibroid embolization, WHO = World Health Organization

TEACHING POINTS

- In the FIGO classification system, numbers are used to categorize the location of leiomyomas. Given that this classification is meant to aid in the workup of abnormal uterine bleeding, submucosal leiomyomas (FIGO stages 0–2) are differentiated from other leiomyomas that do not involve the endometrium (FIGO stages 3–8).
- Bleeding, calcification, and necrosis due to decreased vascular supply are common in degenerated leiomyomas. However, these tumors maintain a circumscribed border and have no cellular necrosis on pathologic specimens; these findings can manifest as T1-hyperintense areas on MR images.
- Leiomyosarcoma classically appears as a new or enlarging solid uterine mass with intermediate to high T2 signal intensity, high T1 signal intensity, and central nonenhancing regions with irregular margins in postmenopausal women.
- Extrauterine leiomyomas have imaging characteristics that are similar to those of typical leiomyomas but with atypical locations. As such, radiologist familiarity with uncommon growth patterns is required for an accurate diagnosis, as many of these tumors with uncommon locations may mimic pelvic malignancies.
- Asymptomatic individuals are usually managed expectantly without treatment. For symptomatic patients, the location of the leiomyoma and the patient's desire to maintain fertility are important management considerations.

higher than in other populations) (4). Additional risk factors include early menarche (5); diet elements such as high intake of alcohol, caffeine, and red meat (6); and genetic factors (eg, hereditary leiomyomatosis and renal cell carcinoma syndrome, fumarate hydratase deficiency). A protective factor is increased parity, possibly from increased selective apoptosis of small leiomyomas during pregnancy and the susceptibility of the leiomyoma to infarction (7).

Patients most commonly are asymptomatic or present with acute or chronic conditions, which may include pain, menstrual disorder, subfertility, and symptoms related to mass effects on the bowel or urinary bladder that cause constipation or frequent urination. Clinical management is aimed at reducing symptoms or increasing fertility with interventional and medical options.

US is the first line of imaging in all cases, and it may be sufficient if the findings are uncomplicated, such as when imaging a solid, well-defined, concentric mass and the triage to treatment is clear. US with saline-infusion sonohysterography can be used for precise anatomic localization. This can be sufficient for cases in which the submucosal location must be established if hysteroscopic resection is considered or conservative management is planned. MRI is superior to US for cases of marked uterine enlargement and for identification of submucosal and subserosal leiomyomas, optimizing the treatment strategy and planning. MRI can also be used to evaluate other causes of uterine and pelvic masses, such as adenomyosis and ovarian neoplasms.

Table 1: Types of Smooth Muscle Tumors of the Uterus Based on 2020 WHO Classification

Leiomyoma
Conventional
Subtypes
Cellular
Leiomyoma with bizarre nuclei
Fumarate hydratase deficient
Mitotically active
Hydropic
Apoplectic
Lipoleiomyoma
Epithelioid
Myxoid
Dissecting leiomyoma
Diffuse leiomyomatosis
Intravenous leiomyomatosis
STUMP
Spindle cell
Epithelioid
Myxoid
Metastasizing leiomyoma
Leiomyosarcoma
Conventional (spindle cell)
Epithelioid
Myxoid

Note.—STUMP = smooth muscle tumor of uncertain malignant potential.

In this article, we review leiomyomas, leiomyosarcomas, and other smooth muscle tumors of the uterus, as categorized in 2020 by the World Health Organization (WHO) (8). The MRI features of conventional (usual) leiomyomas and the International Federation of Gynecology and Obstetrics (FIGO) classification of leiomyomas based on their locations are reviewed (9). Leiomyoma subtypes and forms of leiomyoma degeneration that have established MRI features are also reviewed. The features to date that may help distinguish leiomyosarcoma from leiomyoma subtypes and degenerations also are summarized (Table 1).

Leiomyomas

Leiomyomas have a broad range of imaging appearances on MR images. Conventional leiomyomas account for 80%–90% of leiomyomas, while WHO-based leiomyoma subtypes account for the remaining leiomyomas and can be diagnostically challenging (8). Characteristic MRI features are described for some leiomyoma subtypes, such as cellular, hydropic, apoplectic, and myxoid leiomyoma; lipoleiomyoma; and diffuse leiomyomatosis, whereas the remaining subtypes to date have no established diagnostic features on images

Table 2: MRI Features of Leiomyomas

Leiomyoma Category	Histologic Features	MRI Findings
Conventional	Intersecting fascicles of bland spindle cells with cigar-shaped nuclei are found without atypia, necrosis, or mitotic activity	Circumscribed borders Homogeneous Isointensity or low signal intensity on T1W images Low signal intensity on T2W images Early homogeneous enhancement, similar to myometrial enhancement Low signal intensity on ADC maps
Leiomyoma subtypes		
Cellular	Compact smooth muscle cells without intervening collagen	Circumscribed borders Signal intensity higher than that of myometrium on T2W images Marked avid early enhancement Mild diffusion restriction and lower ADC levels than those of typical leiomyomas
Lipoleiomyoma	Benign smooth muscle proliferation associated with mature adipocytes	Circumscribed borders Signal intensity similar to subcutaneous fat signal intensity with all pulse sequences, with no diffusion restriction or central enhancement
Apoplectic leiomyoma	Sudden hemorrhagic infarction leading to coagulative necrosis	Circumscribed borders Peripheral rim of low signal intensity on T2W images and high signal intensity on T1W images due to obstructed veins Lack of contrast enhancement, particularly within the central portion of the mass
Hydropic leiomyoma	Edematous stroma that causes compartmentalization of the smooth muscle cells, resulting in cystic spaces with acellular centers	Circumscribed borders Cystic spaces with well-defined areas of markedly high signal intensity on T2W images and low signal intensity without enhancement on T1W images
Myxoid leiomyoma	Interspersed abundant myxoid matrix	Circumscribed borders Low signal intensity on T1W images High signal intensity on T2W images Areas of heterogeneous enhancement within hypoenhancing mucinous lakes
Leiomyoma degeneration		
Hyaline degeneration	Smooth muscle tumor cells are surrounded by a zone of hyalinized fibrous tissue	Circumscribed borders Areas of hyaline degeneration that are typically isointense on T1W images, have low signal intensity on T2W images, and have less enhancement than the myometrium

Note.—ADC = apparent diffusion coefficient, T1W = T1-weighted, T2W = T2-weighted.

that allow them to be distinguished from other leiomyoma subtypes and smooth muscle tumors of the uterus (Table 2).

Conventional (Usual) Leiomyomas

Conventional leiomyomas represent 80%–90% of all leiomyomas and have the classic imaging appearance on MR images (Fig 1) (10) of a smoothly circumscribed mass with a homogeneous and isointense or mildly hypointense signal relative to the myometrium and skeletal muscle on T1-weighted (T1W) images and characteristic low T2 signal intensity compared with the signal intensity of the normal myometrium (11). A T2-hyperintense rim may be present and could be attributed to edema resulting from obstruction or dilatation of peripheral lymphatic vessels and veins (12).

Although contrast material administration is not necessary for diagnosis, nondegenerated leiomyomas typically show early homogeneous enhancement, similar to the enhancement of the background myometrium.

Leiomyomas have characteristically low signal intensity on diffusion-weighted MR images (13,14) and low signal intensity on apparent diffusion coefficient (ADC) maps owing to the T2 blackout effect caused by an abundance of hyalinized collagen (15). At histologic analysis, intersecting fascicles of bland spindle cells with cigar-shaped nuclei are found without atypia, necrosis, or mitotic activity (Fig 1).

Localization of Leiomyomas

Historically, leiomyomas have been described by using a three-tiered system to indicate their location: submucosal, intramural, or subserosal. With the development of the FIGO classification system (16), more detailed descriptors were applied to aid with treatment planning and response assessment. The FIGO system was devised to classify abnormal uterine bleeding into nine basic categories, with use of the acronym PALM-COEIN (*p*olyp, *a*denomyosis, *l*eiomyoma, *m*alignancy and hyperplasia, *c*oagulopathy, *o*vulatory dysfunction, *e*ndometrial, *i*atrogenic,

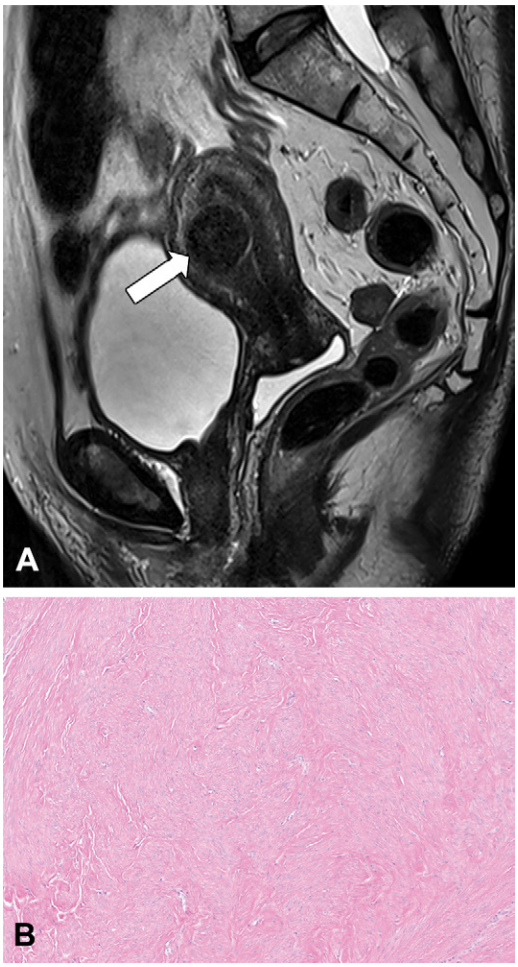

Figure 1. Nondegenerated conventional leiomyoma in a 32-year-old woman. **(A)** Sagittal T2W MR image shows a round T2-hypointense leiomyoma (arrow) of the anterior uterine body (FIGO stage 1). **(B)** The histopathologic specimen from this patient is that of a typical leiomyoma and shows a fascicular growth of bland spindle cells with eosinophilic cytoplasm. (Hematoxylin-eosin [H-E] stain; original magnification, ×100.)

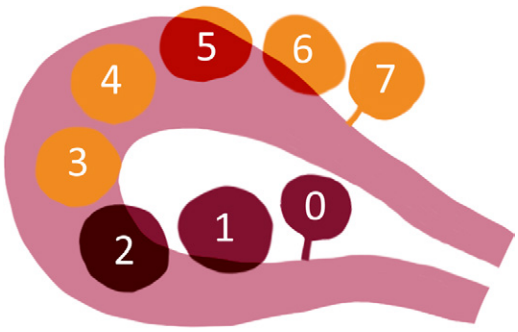

Figure 2. Schematic overview of leiomyoma locations based on FIGO subclassification system. Stage *0* = intracavitary pedunculated, stage *1* = submucosal with less than 50% of tumor being intramural, stage *2* = submucosal with 50% or more of tumor being intramural, stage *3* = intramural with endometrial contact, stage *4* = 100% intramural, stage *5* = subserosal with 50% or more of tumor being intramural, stage *6* = subserosal with less than 50% of tumor being intramural, stage *7* = subserosal pedunculated.

Table 3: FIGO Location-based Subclassifications of Leiomyomas

Category	Stage	Location
Submucosal	0	Intracavitary pedunculated: attached to the endometrium by a narrow stalk (stalk diameter ≤ 10% of the mean diameter of the leiomyoma)
	1	<50% intramural (≥50% submucosal)
	2	≥50% intramural (<50% submucosal)
Other	3	100% intramural but with contact with the endometrium
	4	100% intramural; no submucosal or subserosal components
	5	Subserosal, ≥50% intramural
	6	Subserosal, <50% intramural
	7	Subserosal-pedunculated: attached to the serosa by a narrow stalk (stalk diameter ≤ 10% of the mean diameter of the leiomyoma)
	8	Nonuterine (eg, cervical, parasitic); specific location should be described
Hybrid	#–#	Submucosal and subserosal components; first number denotes the submucosal component, and second number denotes the subserosal component
Additional features to report	...	Total uterine volume
	...	Estimated number of leiomyomas (one, two, three, four, more than four); at minimum, measure largest leiomyoma when there are four or more tumors

and *n*ot yet classified). In the FIGO classification system, numbers are used to categorize the location of leiomyomas (Fig 2, Table 3). Given that this classification is meant to aid in the workup of abnormal uterine bleeding, submucosal leiomyomas (FIGO stages 0–2) are differentiated from other leiomyomas that do not involve the endometrium (FIGO stages 3–8).

The FIGO classification system also accounts for overlap in the locations of "hybrid" leiomyomas with use of a hyphenated designation whereby the first number reflects the relationship to the endometrium and the second number reflects the relationship to the serosa. For example, a leiomyoma whose components are less than 50% submucosal and less than 50% subserosal would be labeled as a FIGO stage 2–5 tumor. The 2018 revision of the FIGO classification includes two additional features: an estimate of the number of leiomyomas (one, two, three, four, or more than four) and an estimate of the total uterine volume based on imaging findings (9). When more than four leiomyomas are present, at minimum, the largest leiomyoma should be measured.

The FIGO system has advanced from the traditional classification that was based only on the relationships of leiomyomas with mucosal surfaces to now include all leiomyomas in relation to both mucosal and serosal surfaces. As management strategies have advanced to include minimally invasive procedural treatments, the FIGO classification system was developed as a universally accepted and widely disseminated

Figure 3. FIGO stage 0 leiomyoma in a 42-year-old woman who presented with heavy menses. Sagittal T2W MR image shows a hypointense pedunculated conventional leiomyoma (arrow) extending from the lower uterine segment into the upper vagina. The thin stalk (arrowhead) can be seen within the endocervical canal. There is also a FIGO stage 1 submucosal leiomyoma partially imaged in the superior aspect of the endometrium.

classification system across subspecialties. Assessment of the leiomyoma location is important, as misclassifying the location of a leiomyoma could lead to treatment complications. For example, if a FIGO stage 0 or 1 leiomyoma were embolized, it could result in the leiomyoma passing through the cervix, resulting in infection or pain. In the setting of myomectomies, resection of a leiomyoma with a greater than 50% extension into the myometrium would increase the risk of bleeding, adhesions, or uterine rupture.

Limitations of the FIGO classification system include interobserver variability in FIGO staging, especially in the staging of large leiomyomas, with increased volume associated with more discrepancies (17). Larger leiomyomas result in greater distortion of uterine landmarks, leading to difficulty assessing myometrial extension (17). As misclassifications can result in inappropriate surgical planning, it may be helpful for the radiologist to review the imaging findings with the gynecologic team before surgery (18).

Submucosal Leiomyomas.—Although submucosal (FIGO stages 0–2) leiomyomas occur less frequently (5% prevalence), they are the most disruptive, cited as a major cause of abnormal uterine bleeding, infertility, and recurrent pregnancy loss (19). If fertility is desired, these leiomyomas require treatment, regardless of their size. Anatomically, submucosal lesions are located beneath the mucosa and subdivided into three additional categories, depending on the extent of their intramural depth (Table 2). FIGO stage 0 leiomyomas may be at risk for prolapse, depending on their craniocaudal location in the uterus and the length of the stalk (Fig 3).

Other Leiomyomas.—All other (FIGO stages 3–8) leiomyomas, which are without submucosal components, are classified under the category of "other." These include common intrauterine intramural leiomyomas and the rarer extrauterine leiomyomas (Table 2). The symptoms from tumors in these leiomyoma categories are most often related to their large size (bulk symptoms), which results in mass effect on adjacent structures such as the bowel and bladder.

Subserosal leiomyomas, FIGO stages 6 and 7 in particular, may be difficult to distinguish from adnexal or other pelvic (rather than a primary uterine) masses. In this setting, the identification of bridging vessels between the uterus and the mass indicates a uterine origin of the mass and a confident diagnosis of leiomyoma (20). On T2-weighted (T2W) MR images, bridging vessels appear as curvilinear signal voids (Fig 4), and on postcontrast MR images, a claw sign with the adjacent uterine tissue should be carefully examined. The pedunculated morphology of these leiomyomas places them at risk for torsion (Fig 5) and detachment into the peritoneum.

Leiomyoma Subtypes

Cellular Leiomyomas.—Significantly more cellular than the normal myometrium, cellular leiomyomas have a soft cut surface showing a tan to yellow color. Microscopically, they have cellular density that is typically seen in endometrial stromal neoplasms but without cytologic atypia or increased mitotic activity (fewer than four mitoses per square millimeter). Large thick-walled vessels are often present throughout the tumor.

At imaging, cellular leiomyomas tend to appear as a single large uterine mass with higher signal intensity than conventional leiomyomas and the myometrium on T2W MR images (Fig 6) (14). The T2 hyperintensity of cellular leiomyomas reflects fluid-rich tissues that have abundant blood vessels, with avid early enhancement compared with the myometrium and earlier enhancement than conventional leiomyomas (14). Their hypercellularity can result in mild diffusion restriction relative to the myometrium, with lower ADC levels than typical leiomyomas (21). In the study by Tasaki et al (21) involving 168 lesions, the ADC values for the two cellular leiomyomas were 0.92×10^{-3} mm^2/sec and 0.75×10^{-3} mm^2/sec, while the mean ADC for leiomyomas was 1.30×10^{-3} mm^2/sec. Compared with leiomyosarcomas, cellular leiomyomas are typically more homogeneous in appearance and enhancement, with no necrosis (14).

Lipoleiomyoma.—Leiomyomas containing a variable amount of mature adipocytes admixed with smooth muscle cells are referred to as lipoleiomyomas (Fig 7), which are usually found in postmenopausal patients. The fat is not the result of degeneration but rather of fatty metaplasia of smooth muscle cells (22). Histopathologic specimens show benign smooth muscle proliferation associated with mature adipocytes (23).

CT shows a well-circumscribed mass containing macroscopic fat (attenuation less than −10 HU to −20 HU). On MR images, the fatty components have signal intensity similar to fat signal intensity with all pulse sequences, with no diffusion restriction or central enhancement. Fat-saturated MR images show suppression of bulk fat in the lesion.

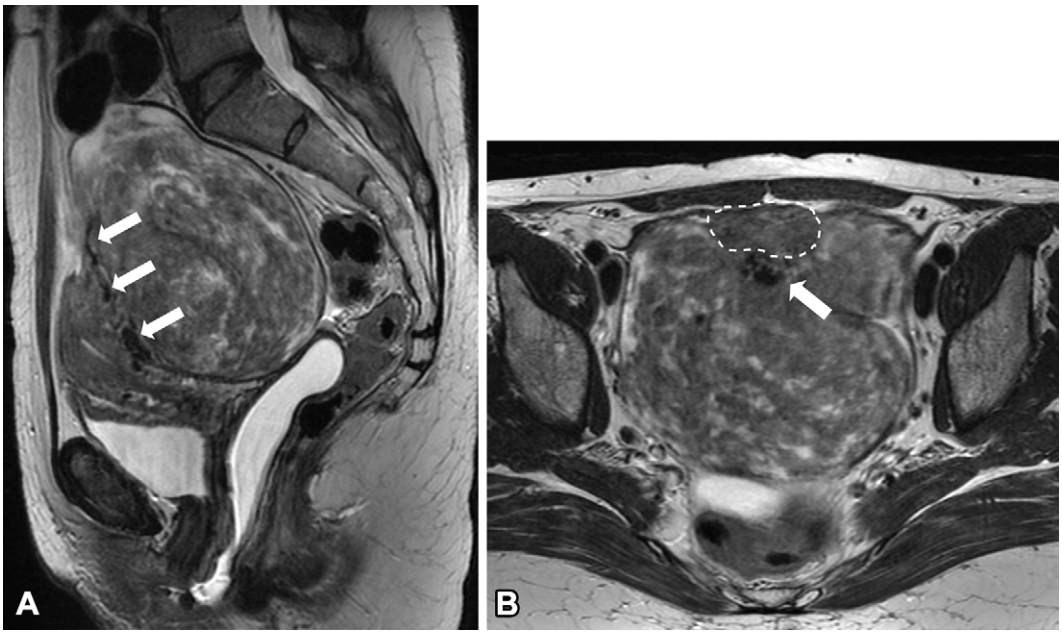

Figure 4. Large exophytic FIGO stage 7 myxoid subserosal leiomyoma in a 38-year-old woman who presented with pelvic pain. **(A)** Sagittal T2W MR image shows a T2 heterogeneous mass with bridging vessels that appear as T2-hypointense flow voids (arrows) between the mass and the posterior uterine body, compatible with their origin from the uterus. **(B)** Axial T2W MR image at the level of approximately the middle arrow in **A** shows the black flow voids, representing the cluster of uterine vessels bridging the uterine fundus anteriorly (arrow, dashed outline) and the leiomyoma posteriorly and laterally.

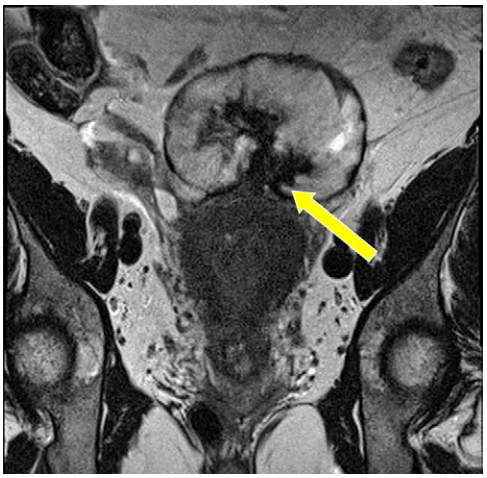

Figure 5. Confirmed torsed fundal FIGO stage 7 exophytic pedunculated leiomyoma in a 31-year-old woman who presented with acute-onset pelvic pain. Coronal T2W MR image shows a T2 heterogeneous leiomyoma with central T2 hypointensity in a corkscrew configuration, corresponding to the twisted pedicle (arrow). The T2-hypointense twisted portion is contiguous with the myometrium.

Apoplectic Leiomyoma.—The apoplectic leiomyoma subtype is associated with red or hemorrhagic degeneration (24), which is also referred to as carneous degeneration. On gross pathologic specimens, there is classically a mottled dark red appearance (25), which is due to sudden hemorrhagic infarction from thrombosis of peripheral drainage veins, leading to coagulative necrosis (25). The histopathologic description is that of ischemia or infarct. This type of degeneration has historically been associated with pregnancy or oral contraceptive use, and patients classically present with acute lower abdominal pain. The degeneration associated with apoplectic leiomyoma is distinct from other types of degeneration owing to the possible systemic manifestations of fever and leukocytosis, which pose a diagnostic dilemma in pregnant patients because of the overlap in symptoms with other acute processes such as appendicitis and cholecystitis.

Acute and chronic cases can have different imaging appearances, depending on the stage of hemorrhage. The apoplectic leiomyoma subtype most commonly demonstrates diffuse high signal intensity on T1W MR images, with variable appearances, ranging from hyperintensity to hypointensity, on T2W MR images (26). At MRI, there is often a distinct peripheral rim of low T2 signal intensity (27) and a rim of high T1 signal intensity (Fig 8), reflecting thrombosed peripheral vessels. At contrast-enhanced MRI, there is a lack of enhancement, particularly within the central portion of the mass, due to a loss of blood supply.

Hydropic Leiomyoma.—Hydropic degeneration, also referred to as cystic degeneration, is a rare subtype characterized by a prominent edematous stroma that causes compartmentalization of the smooth muscle cells (8), resulting in cystic spaces with acellular centers (10). These cystic spaces may be appreciated at imaging. MR images show well-defined areas of fluid signal intensity, which appear as marked T2 hyperintensity and T1 hypointensity without enhancement (Fig 9).

Myxoid Leiomyoma.—At pathologic analysis, myxoid leiomyoma is defined by a well-circumscribed smooth muscle tumor

Figure 6. Cellular leiomyoma found in a 38-year-old woman who presented for evaluation of severe menorrhagia. **(A)** Axial T2W MR image shows a large left uterine body leiomyoma (arrows) with slightly greater T2 signal intensity compared with the myometrium and other leiomyomas of the uterus *(f)*. **(B)** Sagittal early postcontrast T1W fat-saturated MR image shows greater enhancement of the cellular leiomyoma (arrow) compared with the myometrium and other usual leiomyomas. **(C, D)** Axial diffusion-weighted MR image **(C)** and ADC map **(D)** show the cellular leiomyoma (arrow), with hyperintensity in **C** and corresponding low ADC signal intensity (measured region-of-interest [ROI] ADC, 0.945 × 10^{-3} mm^2/sec) in **D**. Intraoperatively, the cellular leiomyoma demonstrated a softer consistency than the other leiomyomas. **(E)** Photomicrograph shows the cellular tumor to be composed of cellular spindle cell proliferation without eosinophilic cytoplasm. The thick-walled vessels at the periphery (arrows) are characteristic of cellular leiomyoma. (H-E stain; original magnification, ×200.)

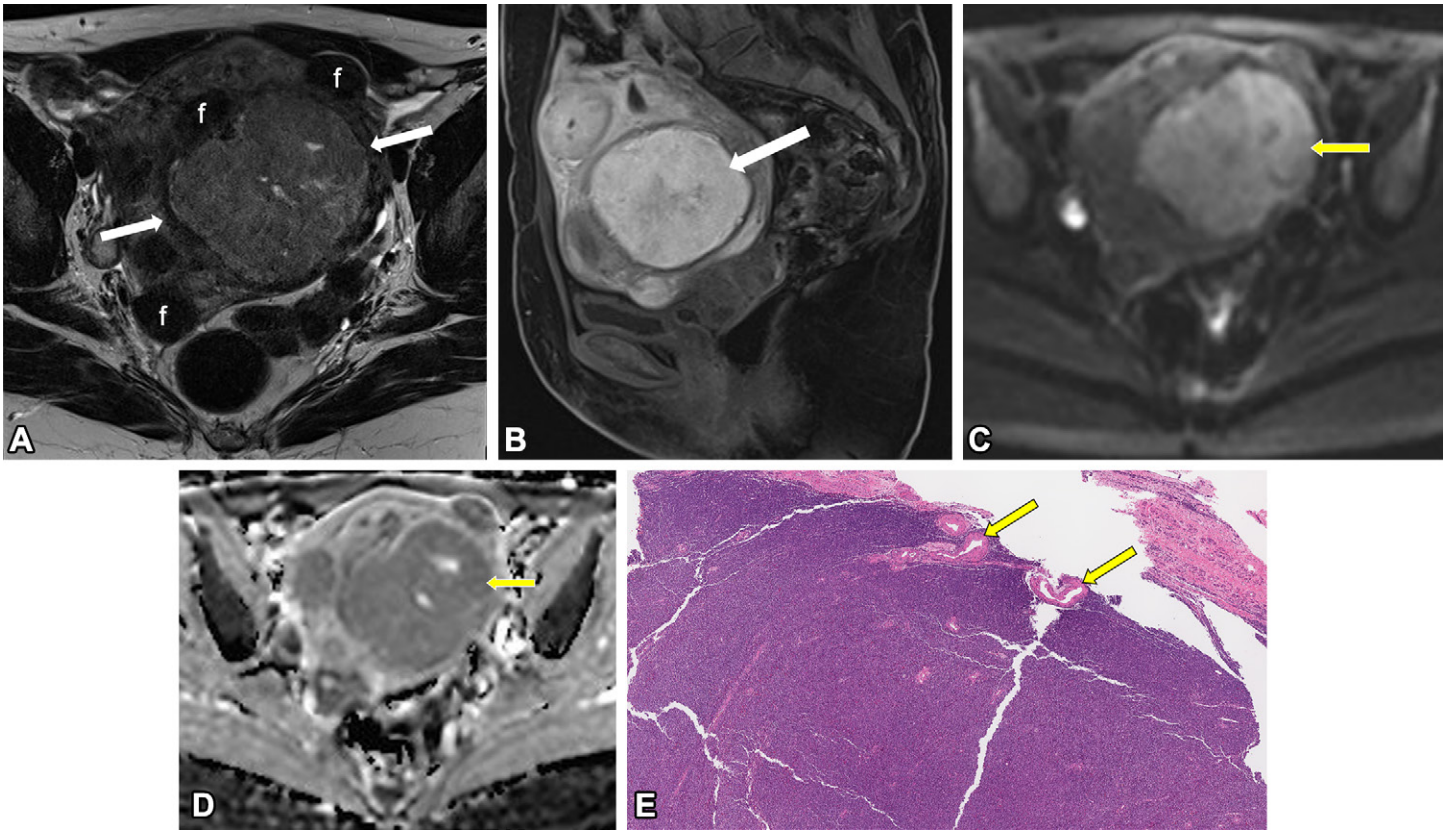

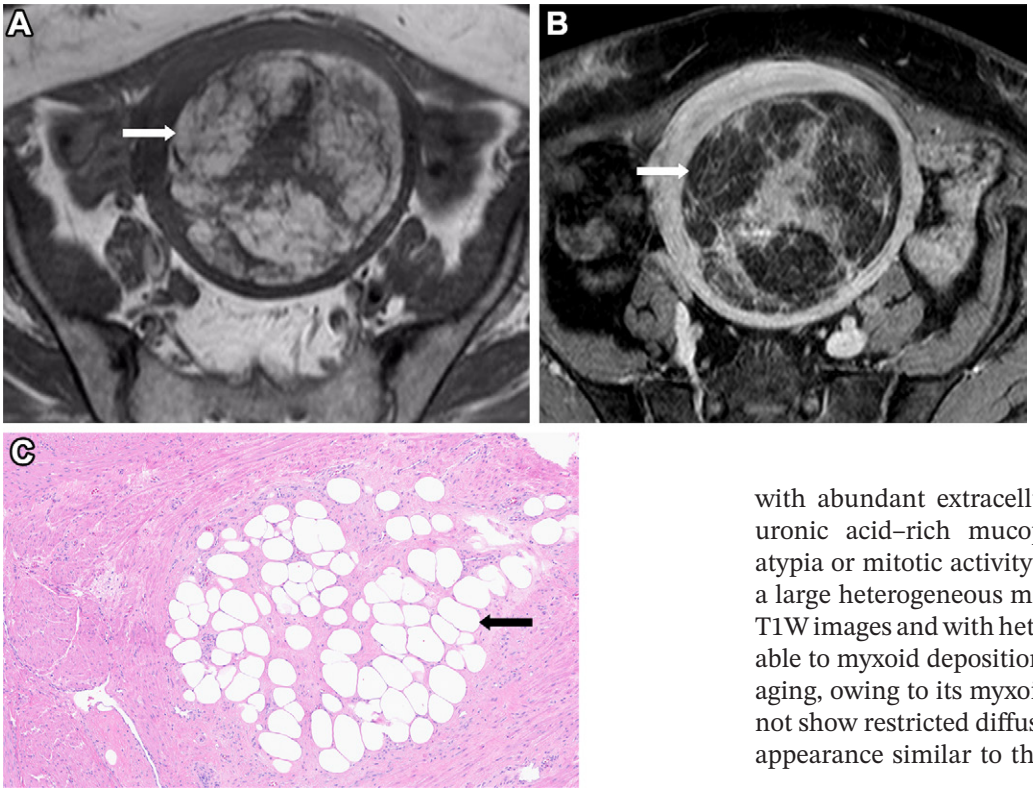

Figure 7. New pelvic mass confirmed to be a lipoleiomyoma in a 49-year-old woman. **(A)** Axial T1W MR image shows a large uterine mass with heterogeneous signal intensity, including many locules of T1 hyperintensity, particularly along the periphery of the mass (arrow). **(B)** Axial postcontrast T1W fat-saturated MR image shows corresponding suppression of T1 hyperintensity within the mass (arrow), similar to that in subcutaneous and peritoneal fat, compatible with bulk fat. **(C)** Photomicrograph shows benign smooth muscle cells associated with mature adipocytes (arrow). (H-E stain; original magnification, ×200.)

with abundant extracellular stroma myxoid material (hyaluronic acid–rich mucopolysaccharides) without cytologic atypia or mitotic activity (28). At MRI, it typically appears as a large heterogeneous mass that is hypointense to muscle on T1W images and with heterogeneous T2 hyperintensity ascribable to myxoid deposition (Fig 10). At diffusion-weighted imaging, owing to its myxoid contents, myxoid leiomyoma does not show restricted diffusion. These leiomyomas may have an appearance similar to that of cystic degeneration, with high

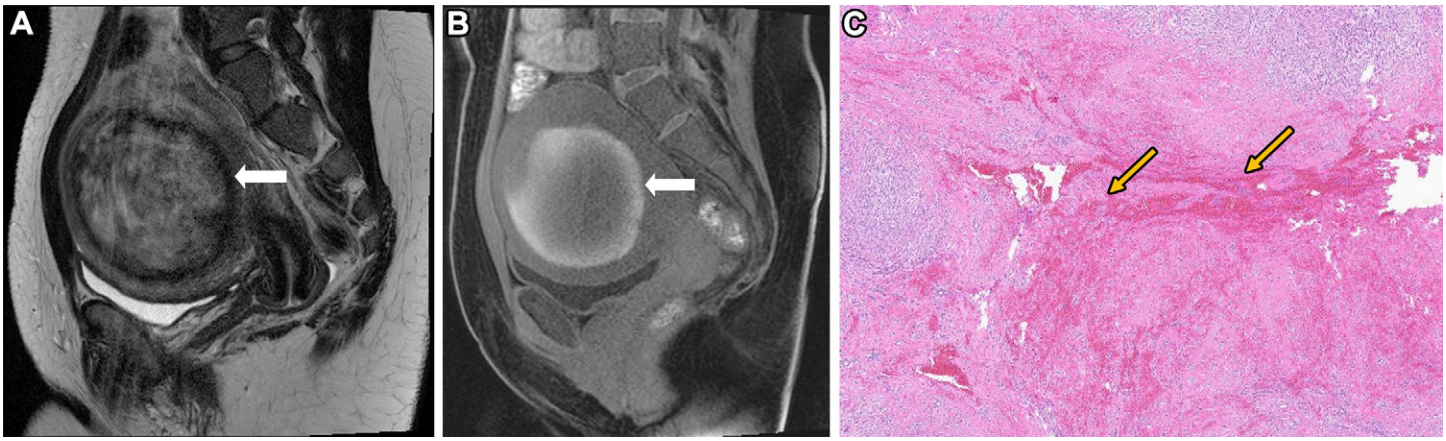

Figure 8. Apoplectic leiomyoma with hemorrhagic degeneration in a 26-year-old woman taking oral contraceptives who presented with acute pelvic pain. **(A)** Sagittal T2W MR image shows heterogeneous T2 signal intensity of a single large leiomyoma with a hypointense rim (arrow). **(B)** Sagittal T1W fat-saturated MR image shows hyperintensity of the leiomyoma (arrow), particularly at the periphery. The leiomyoma showed little enhancement on postcontrast MR images (not shown). **(C)** Histopathologic specimen shows the leiomyoma with ischemia and infarct; the arrows point to a central area of mummified smooth muscle cells and hemorrhage associated with dilated vessels. (H-E stain; original magnification, ×10.)

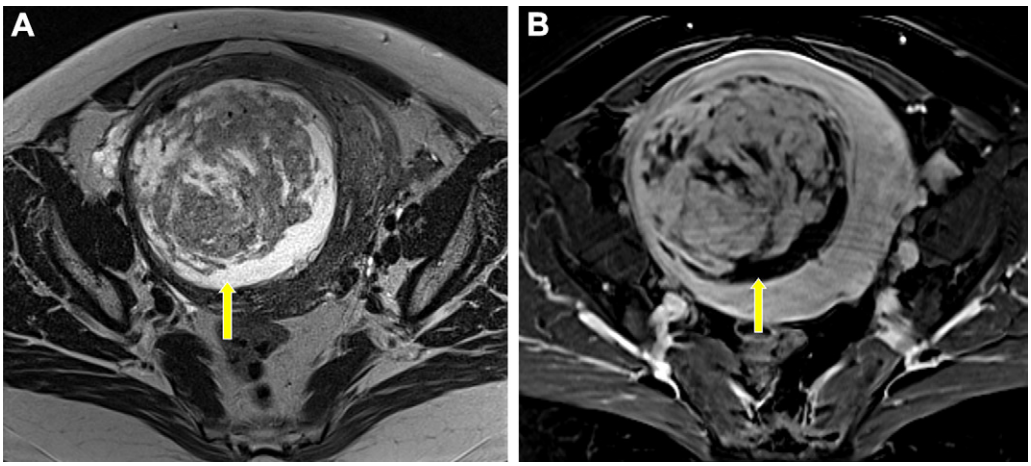

Figure 9. Hydropic leiomyoma in a 51-year-old woman with bulk symptoms, including abdominal bloating, who underwent laparoscopic myomectomy. **(A)** Axial T2W MR image shows a large FIGO stage 5 leiomyoma (arrow) with heterogeneous signal intensity in the right uterine body. There are confluent areas of T2 hyperintensity, particularly along the periphery of the tumor. **(B)** Corresponding axial postcontrast T1W fat-saturated subtraction MR image shows a well-demarcated area lacking enhancement (arrow) in the regions of the leiomyoma with T2 hyperintensity, compatible with hydropic leiomyoma.

T2 signal intensity; however, there are areas of heterogeneous enhancement within the hypoenhancing myxoid lakes and no obvious central nonenhancing necrotic component. The MRI signal intensity features of myxoid leiomyomas may overlap with those of myxoid-type leiomyosarcomas.

Leiomyoma Degeneration

Leiomyomas can undergo one or several types of degeneration that may alter their imaging appearance. In a pathologic study involving 298 patients, degeneration was demonstrated in 65% of specimens (25). As leiomyomas enlarge, the likelihood of degeneration increases. Additional causes of degeneration can include trauma, postmenopausal atrophy, and prior therapy changes such as uterine fibroid embolization (UFE). Bleeding, calcification, and necrosis due to decreased vascular supply are common in degenerated leiomyomas. However, these tumors maintain a circumscribed border and have no cellular necrosis on pathologic specimens; these findings can manifest as T1-hyperintense areas on MR images.

The most common form of leiomyoma degeneration is hyaline degeneration, whereby smooth muscle is replaced by collagen, which is present in up to 60% of leiomyomas (29). At histopathologic analysis, there is hyalinization of the stromal component with collection of proteinaceous tissue, leading to homogeneous eosinophilic bands (30). Ghost outlines of typical smooth muscle cells are surrounded by a zone of hyalinized fibrous tissue. At MRI, areas of hyaline degeneration typically enhance less than the myometrium while appearing isointense on T1W images and hypointense on T2W images (Fig 11). These findings are in contrast to those of a typical leiomyoma, which, similar to the myometrium, demonstrates early homogeneous enhancement. Hemorrhagic, cystic, and myxoid degeneration of leiomyomas is also possible and may satisfy additional histopathologic criteria to be subtyped as apoplectic, hydropic, and myxoid leiomyoma, respectively, in the 2020 WHO 2020 classification of smooth muscle tumors. However, these forms of degeneration may also be found histopathologically within a leiomyoma without meeting the criteria for a specific leiomyoma subtype (8).

Intravenous Leiomyomatosis

Intravenous leiomyomatosis is an intravascular growth of smooth muscle cells in the absence of or beyond the confines of a leiomyoma, sometimes with pelvic or even extrapelvic

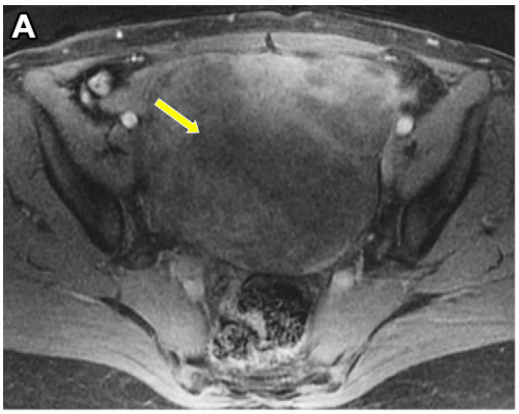

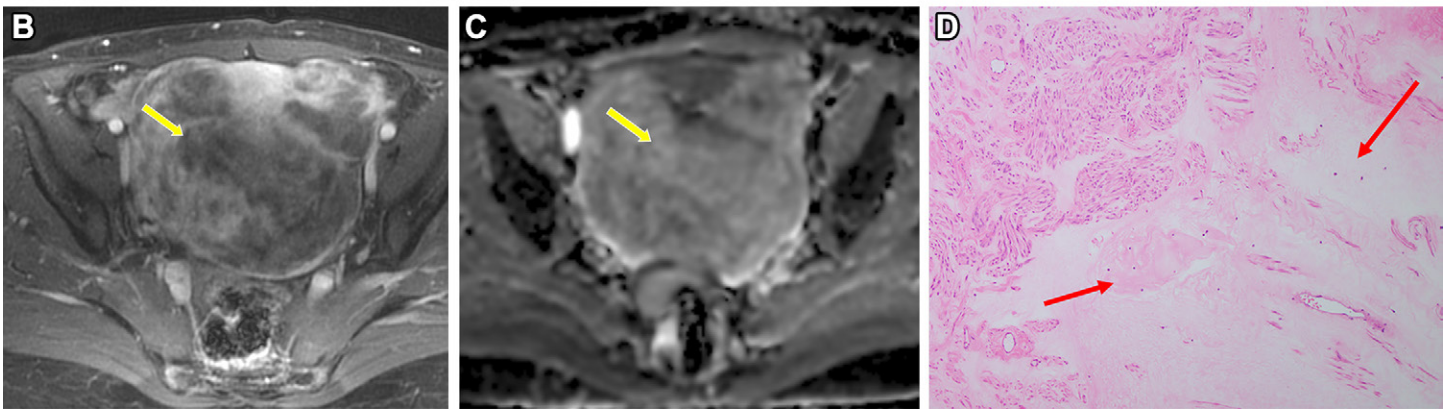

Figure 10. Long-standing pelvic mass, with new myxoid degeneration compatible with myxoid leiomyoma (ML), in a 38-year-old woman. **(A, B)** Axial precontrast **(A)** and postcontrast **(B)** T1W fat-saturated MR images show hypointensity of the myxoid leiomyoma (arrow), with corresponding heterogeneous hypoenhancement. There are no clearly demarcated regions of nonenhancement within the ML owing to the presence of mucinous lakes, which show hypoenhancement. **(C)** Axial ADC map shows no significant areas of diffusion restriction (arrow) (region-of-interest ADC, 1.888 $\times 10^{-3}$ mm^2/sec). Figure 4 shows corresponding T2W MRI findings in this patient. **(D)** Histopathologic specimen shows abundant myxoid matrix. The smooth muscle cells are benign appearing, and the area of smooth muscle proliferation is well demarcated from the myxoid matrix. Arrows point to the areas of myxoid degeneration. (H-E stain; original magnification, ×100.)

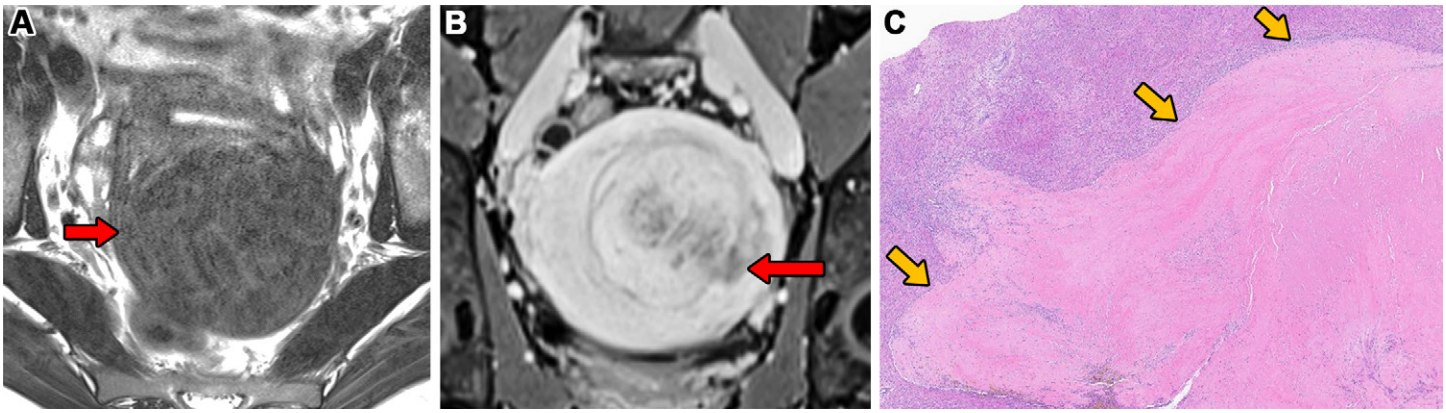

Figure 11. Confirmed leiomyoma with hyaline degeneration in a 34-year-old woman with a history of pelvic pain. **(A)** Axial T2W MR image shows a leiomyoma (arrow) with relatively uniform hypointensity, as is typically seen with these tumors. **(B)** Coronal postcontrast T1W fat-saturated MR image shows mildly heterogeneous enhancement of the leiomyoma, which was T1 isointense on the precontrast MR image (not shown). Areas of hyaline degeneration (arrow) are shown to enhance less than the adjacent myometrium. **(C)** Histopathologic specimen shows the leiomyoma with hyaline degeneration. (H-E stain; original magnification, ×100); arrows show the clear demarcation between the leiomyoma and the hyaline zone (light pink area).

extension. It is characterized by the presence of bland smooth muscle cells within veins of the uterus or systemic veins (Fig S1), from implants of previously resected or concurrent leiomyomas. There are several case reports of leiomyomatosis extending to the right atrium, which may result in fatal obstruction. The signal intensity of the smooth muscle within the veins typically reflects that of the uterine leiomyoma and therefore may be variable, but the morphologic appearance is that of wormlike expansion in the pelvic veins (31). Pathologically, this entity is defined by the presence of benign smooth muscle cells that resemble conventional leiomyoma or one of the leiomyoma subtypes within vascular spaces—usually veins, or less commonly lymphatic spaces, but not arteries. There is generally a significant risk of recurrence, even many years after surgical resection (32). The differential consideration is leiomyosarcoma of the inferior vena cava, which cannot be differentiated on the basis of imaging findings unless there is abdominal solid-organ invasion.

Smooth Muscle Tumors of Uncertain Malignant Potential

In the WHO classification, smooth muscle tumors of uncertain malignant potential (STUMP) are designated as uterine smooth muscle tumors that are not unequivocally benign or

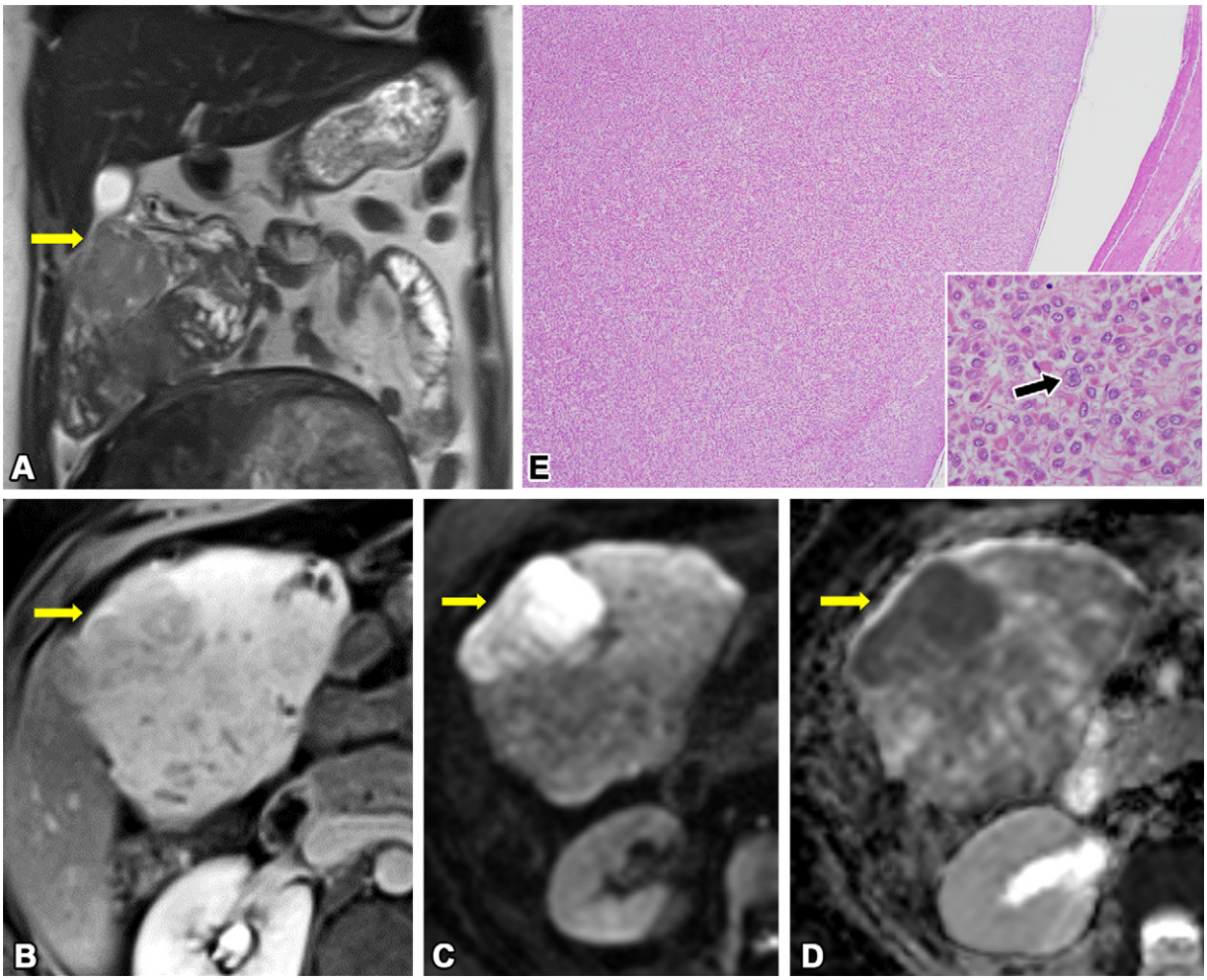

Figure 12. Multiple pelvic masses, including a STUMP tumor and multiple leiomyomas, in a 36-year-old woman with bulk symptoms, including abdominal fullness. **(A)** Coronal T2W MR image shows a heterogeneously hyperintense right upper quadrant subserosal FIGO stage 7 uterine mass (arrow), which was found to be a STUMP tumor at pathologic analysis. Additional intramural uterine masses, consistent with leiomyomas, are partially visualized. **(B)** Axial postcontrast T1W fat-saturated MR image shows avid heterogeneous arterial phase hyperenhancement of the mass (arrow), which was hypointense on precontrast MR images (not shown). **(C, D)** Axial diffusion-weighted **(C)** and ADC **(D)** MR images show the mass (arrow) with avid diffusion restriction in **C** and corresponding ADC hypointensity in the right anterior aspect of the mass in **D**. The region-of-interest (ROI) ADC measurement in the enhancing, more T2-hyperintense, darker ADC portion of the mass is 0.863 × 10^{-3} mm^2/sec. **(E)** Histopathologic specimen shows a well-circumscribed myometrial mass with cellular epithelioid cell proliferation, with no necrosis identified. (H-E stain; original magnification, ×40.) The tumor is predominantly composed of epithelioid smooth muscle cells with eosinophilic cytoplasm, with moderate cytologic atypia (arrow in inset [H-E stain; original magnification, ×400]), consistent with a STUMP tumor.

malignant at histologic analysis. STUMP should not be used histopathologically as a "waste bucket"–type diagnosis (Fig 12). Uterine smooth muscle tumors with one of the following features are usually regarded as STUMP: *(a)* no other worrisome features except tumor cell necrosis; *(b)* moderate to severe cytologic atypia and an uncertain mitotic count or necrosis of uncertain type; or *(c)* multifocal or diffuse, moderate to severe cytologic atypia and six to nine mitotic figures per 10 high power fields but no tumor cell necrosis (33).

Differentiation between STUMP, leiomyoma, and leiomyosarcoma is difficult due to overlapping imaging features. Central nonenhancing pockets that are T2 hyperintense are more commonly seen with STUMP and leiomyosarcoma than with leiomyoma (34). The solid component of STUMP tends to exhibit diffusion restriction (35) (Fig 12). Given the overlap in imaging appearances between STUMP and frank uterine malignancies, patients with STUMP typically undergo hysterectomy. For unsuspected tumors diagnosed at pathologic analysis, patients require imaging surveillance if myomectomy was performed instead of hysterectomy, as 5%–30% of STUMPs will metastasize or recur locally in an aggressive fashion (33).

Metastasizing Leiomyoma

Metastasizing leiomyoma is recognized in the WHO classification of uterine smooth muscle tumors and is classified separately from leiomyoma, leiomyosarcoma, and STUMP. It is characterized by the hematogeneous metastasis of leiomyomas to extrauterine sites in patients who have a history of uterine leiomyomas, often with a history of hysterectomy (36). The most common location of leiomyoma metastasis is the lungs (Fig S2). These metastases may manifest as single or multiple smoothly marginated nodules with occasional

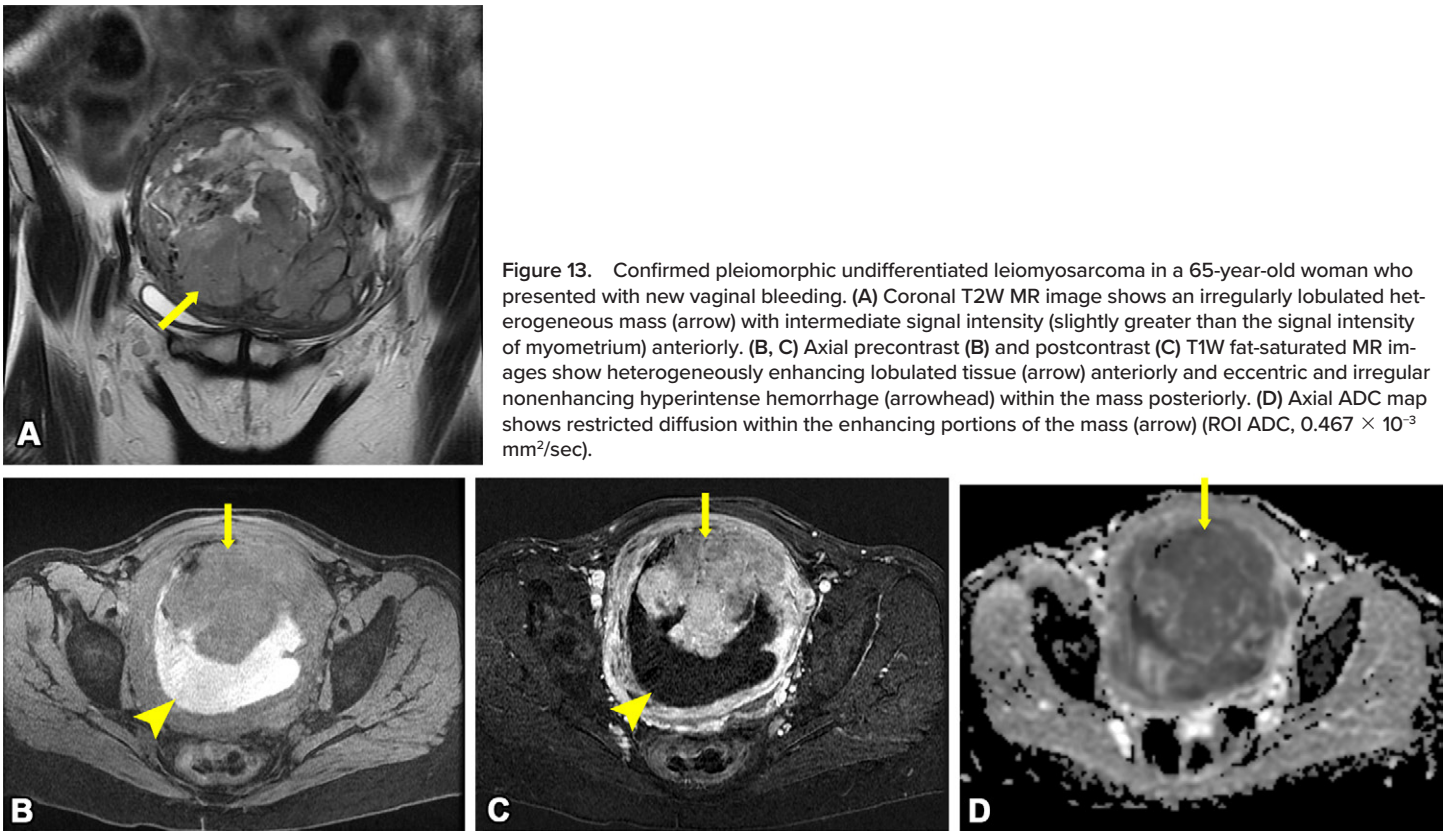

Figure 13. Confirmed pleiomorphic undifferentiated leiomyosarcoma in a 65-year-old woman who presented with new vaginal bleeding. **(A)** Coronal T2W MR image shows an irregularly lobulated heterogeneous mass (arrow) with intermediate signal intensity (slightly greater than the signal intensity of myometrium) anteriorly. **(B, C)** Axial precontrast **(B)** and postcontrast **(C)** T1W fat-saturated MR images show heterogeneously enhancing lobulated tissue (arrow) anteriorly and eccentric and irregular nonenhancing hyperintense hemorrhage (arrowhead) within the mass posteriorly. **(D)** Axial ADC map shows restricted diffusion within the enhancing portions of the mass (arrow) (ROI ADC, 0.467 × 10^{-3} mm^2/sec).

cavitation. Patients are typically asymptomatic, and the clinical course is indolent (37). The differential diagnosis includes pulmonary metastases, with biopsy often required for a definitive diagnosis. Spontaneous resolution of these metastatic leiomyomas has been described in the literature (38).

Leiomyosarcoma

Leiomyosarcoma is defined as a malignant, highly aggressive mesenchymal neoplasm of smooth muscle lineage. The 5-year survival rate in patients who have this malignancy with metastases is 10%–15% (39). At pathologic analysis, these neoplasms have prominent nuclear atypia, areas of geographic coagulative tumor cell necrosis, and 10 or more mitoses per 10 high power fields. There are three main morphologic types of leiomyosarcoma: conventional (spindle cell), epithelioid, and myxoid. Leiomyosarcomas account for less than 1% of uterine tumors but are the most common type of uterine sarcoma, and it can be difficult to differentiate them from leiomyoma subtypes and degeneration, from both a clinical and an imaging perspective. Owing to overlapping features, up to 0.28% of surgically resected presumed benign leiomyomas are diagnosed as leiomyosarcoma at pathologic analysis (40).

The clinical characteristics of leiomyosarcoma are nonspecific, overlapping with those of leiomyoma, and include bleeding, palpable pelvic masses, and pelvic pain (41). Demographic risk factors for leiomyosarcoma include Black race, in whom there is a twofold higher incidence compared with the incidence among White persons (42,43), and postmenopausal status, with age older than 50 years conferring a more than four times greater incidence (42). Most of these tumors arise de novo, with a rare subset of them arising from existing leiomyoma through malignant transformation (44). Therefore, in a postmenopausal patient, a new or enlarging uterine mass should raise concern for leiomyosarcoma (Fig 13) (45,46).

Elevated levels of serum markers such as lactate dehydrogenase (LDH) and cancer antigen 125 (CA-125) were initially believed to be predictors of leiomyosarcoma. However, these markers are nonspecific. LDH, an enzyme in the glycolytic pathway, is associated with higher expression in cancer cells and can be elevated in many cancers, including leiomyosarcoma, breast cancer, and hepatocellular carcinoma (47). However, LDH levels may also be elevated in leiomyomas (48). Elevated CA-125 levels can be seen in 1%–2% of healthy individuals (49) or with other conditions including menstruation, endometriosis, pregnancy, and conditions resulting in peritoneal inflammation (47).

Since leiomyomas can be managed expectantly or with minimally invasive treatments, a missed diagnosis of leiomyosarcoma could result in adverse treatment delays or worse oncologic outcomes. These factors emphasize the importance of preprocedural imaging and the role of the radiologist in identifying leiomyosarcoma or raising suspicion before treatment, which could ensure that leiomyosarcoma dissemination or a delayed diagnosis is avoided. In recent years, there has been renewed interest in the preoperative differentiation of leiomyoma from leiomyosarcoma, especially given the changing advice on morcellation.

The technique of morcellation can be used in both open and minimally invasive surgical approaches, with the goal of reducing a large leiomyoma to smaller pieces for ease of

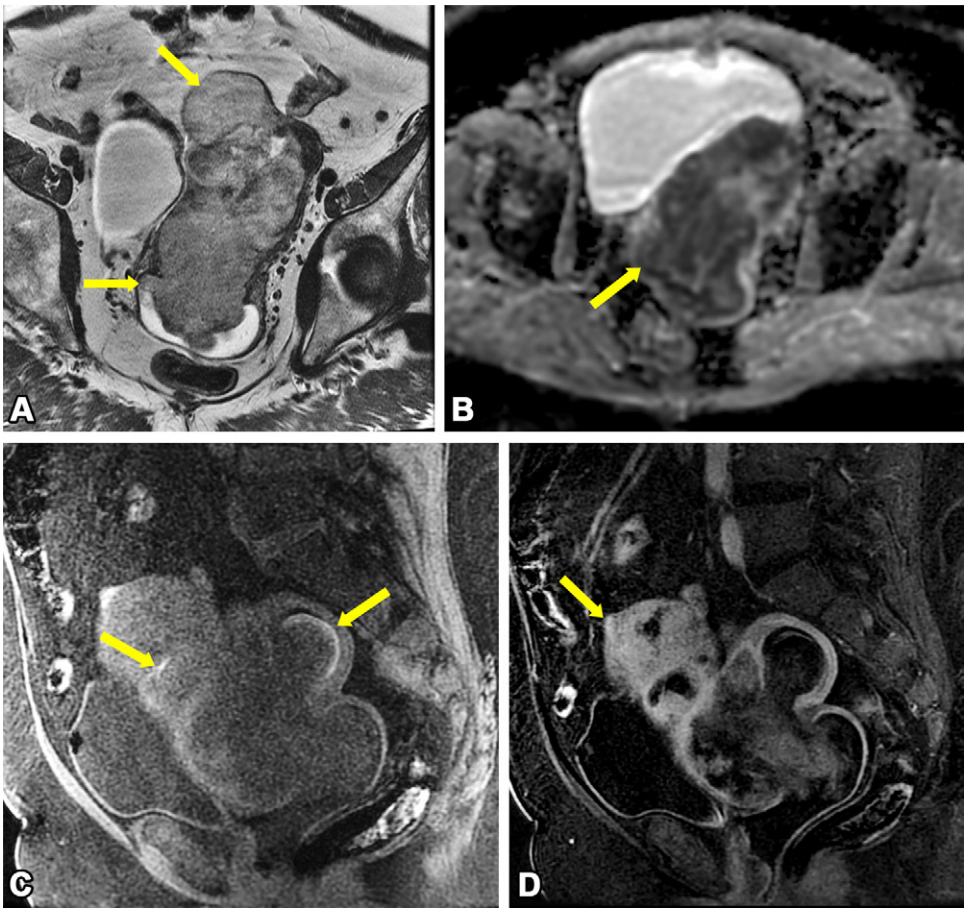

Figure 14. Uterine mass found to be leiomyosarcoma in a 57-year-old woman who underwent MRI for evaluation of a fibroid uterus. **(A)** Axial T2W MR image shows a multilobulated myometrial mass (arrows) with heterogeneous hyperintensity, extending inferiorly to replace the cervix and invade the superior vagina. **(B)** Axial ADC map shows heterogeneous diffusion restriction in the mass (arrow) (ROI ADC, 0.609 × 10^{-3} mm^2/sec). **(C)** Sagittal precontrast T1W fat-saturated MR image shows scattered crescentic hyperintensity (arrows) at the periphery of the lobulated mass due to hemorrhage or necrosis. **(D)** Sagittal postcontrast T1W fat-saturated subtraction MR image shows heterogeneous enhancement in mainly the superior part of the mass (arrow).

removal through a small incision (50). In 2014, the U.S. Food and Drug Administration deemed the use of laparoscopic power morcellators to be contraindicated and advised discussions with the patient regarding the risk of disseminating an unsuspected leiomyosarcoma (51). This decision was made after a highly publicized case of disseminated leiomyosarcoma following a laparoscopic hysterectomy performed with open morcellation (52). Subsequent to these recommendations, many institutions have discouraged the use of morcellation, resulting in a decrease in minimally invasive hysterectomies and increased rates of complications (53,54).

Since 2020, the FDA's recommendation for the use of power morcellators has been reinstated, with the inclusion of guidelines to use a containment system in which tissue is directly placed into a plastic pouch within the peritoneal cavity, as open (uncontained) approaches increase the risk of tissue dissemination (55). Therefore, risk stratification before surgery is needed to optimize minimally invasive surgeries for the majority of leiomyomas, with open hysterectomy reserved for suspected leiomyosarcoma.

US is often the first imaging modality used; however, it does not enable reliable tumor differentiation, as there is significant overlap in the imaging characteristics of leiomyoma and leiomyosarcoma, with the latter generally appearing as a large inhomogeneous mass distorting the uterine architecture, with hemorrhage and necrosis (56).

Due to superior soft-tissue characterization, a large field of view, and multiplanar sequences, MRI is the most accurate modality for characterization of uterine masses. Leiomyosarcoma classically appears as a new or enlarging solid uterine mass with intermediate to high T2 signal intensity, high T1 signal intensity, and central nonenhancing regions with irregular margins in postmenopausal women (Figs 13, 14; Table 4) (57,58).

High T2 signal intensity of the leiomyosarcoma, as compared with the signal intensity of the background myometrium, may be a marker of increased tissue cellularity (Fig S3) (59). This can be seen in leiomyosarcomas, STUMPs, and cellular leiomyomas; however, there is overlap in signal intensity between these neoplasms and myxoid or hydropic degeneration. There is a high prevalence (96%) of T2 hyperintensity in both leiomyosarcoma and leiomyoma but a low prevalence (4%) of T2-hypointense leiomyosarcoma (60). Leiomyosarcoma typically demonstrates high T2 signal intensity within the solid viably enhancing portion of the mass (61). In contrast, leiomyoma degeneration also may show high T2 signal intensity but usually without enhancement (59,60). Like myxoid leiomyoma, myxoid leiomyosarcoma, a more aggressive form of leiomyosarcoma, can appear with heterogeneous, multilocular, marked T2 hyperintensity with progressive contrast enhancement. Unlike their benign counterparts, myxoid leiomyosarcomas potentially can be distinguished by diffusion restriction in portions of the mass that demonstrate corresponding T2 hyperintensity and contrast enhancement (Fig 15) (62).

The diffusion-weighted imaging *b* factor and the ADC, measures of cellular density, have been investigated for their usefulness in diagnosing leiomyosarcoma (63–65). Low ADC

Table 4: MRI Features and Clinical Information Used to Differentiate Leiomyosarcoma from Leiomyoma

Leiomyosarcoma Features	Description*
Most concerning features	
T2-intermediate or high T2 signal intensity	T2 signal intensity is similar to or increased compared with signal intensity of background myometrium and should be measured in a region of the solid enhancing portion of the mass
High signal intensity on DW images	On high–*b*-value diffusion-weighted images, signal intensity is equal to or greater than signal intensity of endometrium or lymph nodes in the solid enhancing portion of the mass
Low signal intensity on ADC maps	Reported ADC cutoff values vary among studies; however, a recent retrospective study (67) showed high sensitivity and specificity with use of a cutoff ADC of less than or equal to 0.905×10^{-3} mm²/sec, as endorsed by a recent expert consensus review (66) A small ROI should be placed in the portion of the mass with the lowest signal intensity; in addition, the ROI should be placed in a viable enhancing portion of the mass, avoiding nonviable hemorrhage or necrosis
Peritoneal implants	Rarely seen but high association with malignancy
Pelvic lymphadenopathy	
Postmenopausal status	Age ≥ 50 years (four times greater incidence)
Potentially helpful secondary features	
Irregular margins	The outer border of the mass demonstrates abrupt angular margins, which may be present with or without soft-tissue protrusions into the parenchyma; this can involve only one portion of the mass
Hemorrhage and necrosis	Nonenhancing high–T1-signal-intensity regions with variable T2 signal intensity, typically within the central portion of the mass
Enhancement	Nonspecific; may see hyperenhancement or finger-like projections; however, enhancement is an important parameter to assist with analysis of additional features such as measurements of T2, diffusion-weighted imaging, and ADC values within solid, viable, enhancing portions of the mass

* Numbers in parentheses are reference numbers.

values have been described as concerning for leiomyosarcoma in multiple studies. However, the cutoff ADC among studies ranges from less than 1.23×10^{-3} mm²/sec to less than 0.82×10^{-3} mm²/sec (21,34,45,58,61,63–69). Quantitatively, a small region-of-interest (ROI) ADC measurement of the solid enhancing tissue of less than or equal to 0.905×10^{-3} mm²/sec in the mass region with the lowest signal intensity is strongly associated with leiomyosarcoma, as suggested in a relatively recent retrospective study (67), in which a sensitivity of 88% and specificity of 100% in the validation set were reported. This value has also been suggested as a cutoff ADC in a recent expert consensus review (66).

Qualitatively, the signal intensity of the solid enhancing portion of the mass that is higher than or equal to the signal intensity of the endometrium or lymph nodes on a $b = 1000$ sec/mm² diffusion-weighted image is considered moderate evidence of leiomyosarcoma (34,63–65). An enhancing portion of the mass should be measured, as nonenhancing areas of hemorrhage or cystic portions may also have low ADC values. In addition, one should keep in mind that there is overlap in ADC values between the highly cellular leiomyoma and leiomyosarcoma (63) due to water restriction caused by increased cellularity.

During the past 2 decades, multiparametric MRI has emerged as the most promising approach for differentiating leiomyoma from leiomyosarcoma. A review of the current literature reveals that the features most strongly associated with leiomyosarcoma include *(a)* intermediate to high signal intensity at T2W MRI and *(b)* high signal intensity at high–*b*-value (1000 sec/mm²) diffusion-weighted imaging, with corresponding low signal intensity at ADC mapping (Fig S4) (21,34,45,58,61,63–69). According to a recent expert consensus review (66), the combination of these features potentially yields an accuracy of 88.0%–94.6% for detecting leiomyosarcoma. Although they are uncommonly seen in leiomyosarcomas, peritoneal implants and pelvic lymphadenopathy (heterogeneous T2 signal intensity with a short axis of ≥1 cm) are two additional features that are strongly associated with malignancy (58,67,70).

Additional features that are potentially suggestive of leiomyosarcoma include irregular margins, hemorrhage or necrosis, and enhancement (66). Although irregular margins are frequently cited as a potential feature of leiomyosarcoma, there is a lack of consensus regarding the definition of these margins, and margin descriptors such as *ill defined, nodular,* and *lobulated* have been used across different studies (35,58,61). A recent expert consensus statement (66) suggests a definition for *irregular borders* as the outer border of the mass demonstrating abrupt angular margins, which may be present with or without soft-tissue protrusions into the parenchyma. This finding may be present in only one portion of the mass (66). *Hemorrhage* or *necrosis* is defined as T1 hyperintensity without enhancement, typically within the central portions of the mass (35,58–60,67,68), which is cited as a feature of leiomyosarcoma by a few smaller-scale studies; however, overlap in this feature can be seen with degenerated leiomyomas.

Although hyperenhancement is not limited to leiomyosarcomas, the presence of enhancement is important in the analysis of additional features such as ADC and diffusion measurements in solid, viable, enhancing portions of the

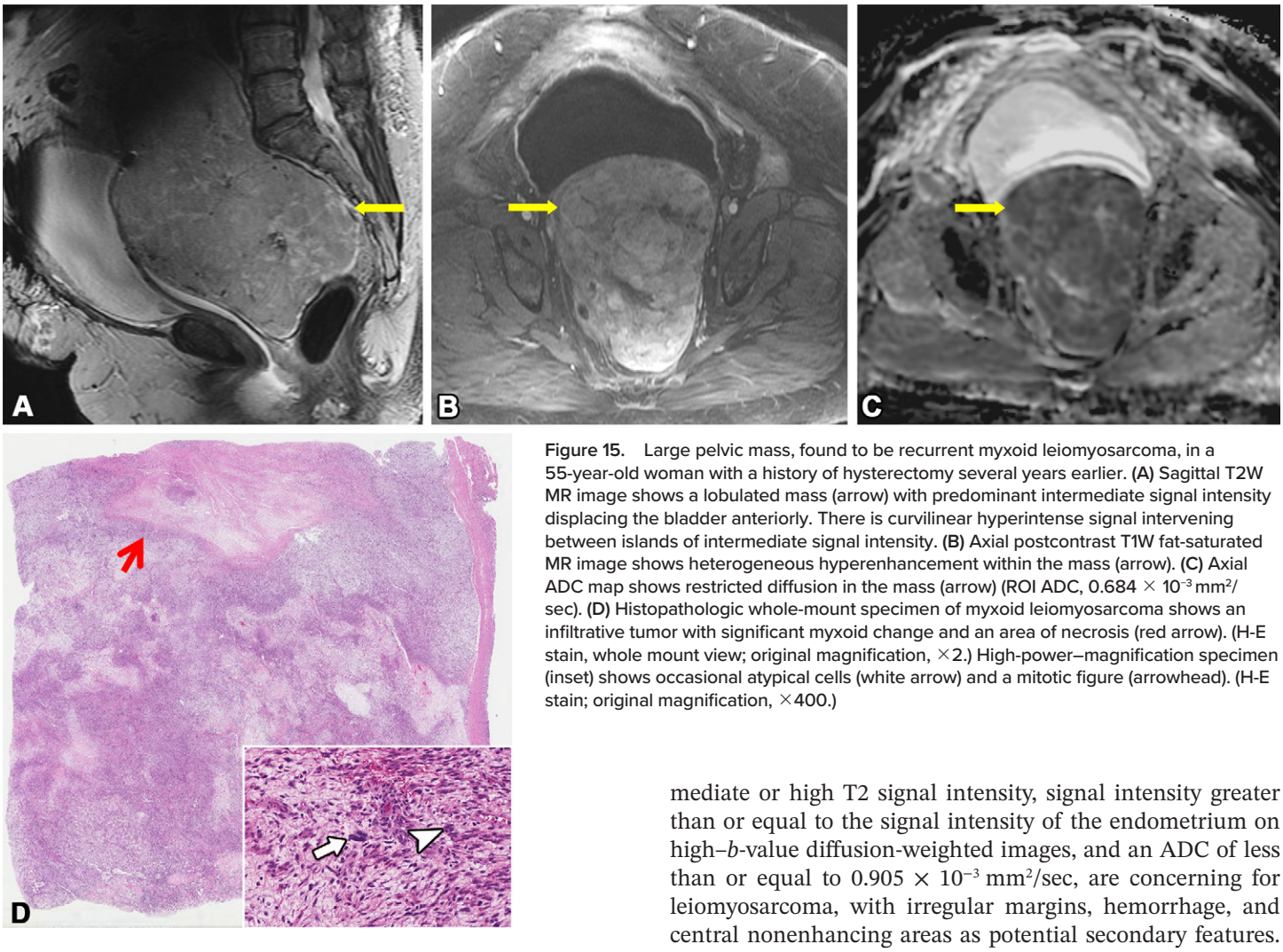

Figure 15. Large pelvic mass, found to be recurrent myxoid leiomyosarcoma, in a 55-year-old woman with a history of hysterectomy several years earlier. **(A)** Sagittal T2W MR image shows a lobulated mass (arrow) with predominant intermediate signal intensity displacing the bladder anteriorly. There is curvilinear hyperintense signal intervening between islands of intermediate signal intensity. **(B)** Axial postcontrast T1W fat-saturated MR image shows heterogeneous hyperenhancement within the mass (arrow). **(C)** Axial ADC map shows restricted diffusion in the mass (arrow) (ROI ADC, 0.684 × 10^{-3} mm^2/sec). **(D)** Histopathologic whole-mount specimen of myxoid leiomyosarcoma shows an infiltrative tumor with significant myxoid change and an area of necrosis (red arrow). (H-E stain, whole mount view; original magnification, ×2.) High-power–magnification specimen (inset) shows occasional atypical cells (white arrow) and a mitotic figure (arrowhead). (H-E stain; original magnification, ×400.)

mass. Finger-like enhancing areas with central nonenhancing pockets of high T2 signal intensity can be seen with leiomyosarcoma, with the nonenhancing areas correlating to cellular necrosis (34,48). This appearance is different from the speckled nonenhancing areas of hyaline degeneration, which are usually smaller and scattered throughout the mass (34). It should be noted that intracavitary masses with finger-like enhancing projections are more commonly seen in high-grade endometrial stromal sarcomas than in leiomyosarcomas, with both mass types managed surgically.

In multiple studies, MRI features have been incorporated into a decision tree for the prediction of leiomyosarcoma, most often with the first determination being whether there is high T2 signal intensity of the solid portion of the mass (60,61,66,71). The signal intensities on diffusion-weighted and ADC images are subsequently examined. Afterward, studies vary in terms of the incorporation of other features, which can include margins, hemorrhage, necrosis, and/or T1 signal intensity. As most of the studies published to date have been retrospective with small sample sizes, future multicenter, prospective, machine-learning, and radiomics studies are required for additional validation.

In summary, a new or enlarging uterine mass in a postmenopausal patient, with a solid enhancing area of intermediate or high T2 signal intensity, signal intensity greater than or equal to the signal intensity of the endometrium on high–*b*-value diffusion-weighted images, and an ADC of less than or equal to 0.905 × 10^{-3} mm^2/sec, are concerning for leiomyosarcoma, with irregular margins, hemorrhage, and central nonenhancing areas as potential secondary features. However, there can be overlap of these features in nonmalignant entities, especially cellular leiomyoma and STUMP. Ultimately, cases should be discussed at multidisciplinary tumor boards, with the patient's age, desire for fertility, and level of concern regarding the MRI features taken into account to guide management.

Other Growth Patterns

Extrauterine leiomyomas have imaging characteristics that are similar to those of typical leiomyomas but with atypical locations. As such, radiologist familiarity with uncommon growth patterns is required for an accurate diagnosis, as many of these tumors with uncommon locations may mimic pelvic malignancies.

Parasitic Leiomyoma

Parasitic leiomyoma is classically described as a pedunculated subserosal leiomyoma that loses its original attachment to the uterus, becoming adherent and sustaining growth through neovascularization from adjacent structures. This is an increasingly recognized complication, seen after morcellation at laparoscopic myomectomy or hysterectomy (72,73), that is due to small residual fragments of leiomyoma implanting in the abdominal cavity and developing an auxiliary blood supply from adjacent structures.

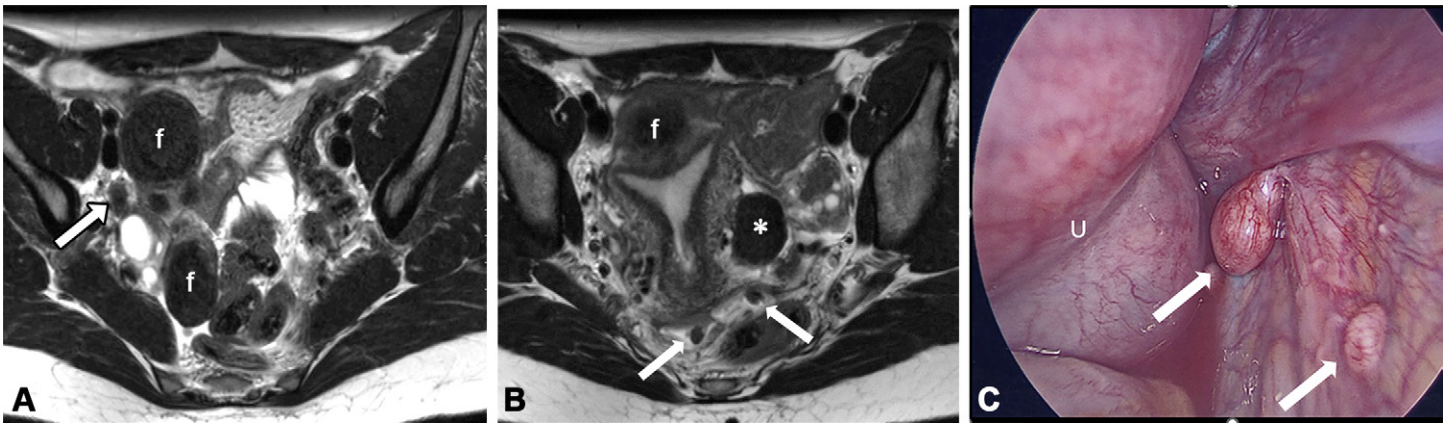

Figure 16. Diffuse peritoneal leiomyomatosis found at workup for infertility in a 40-year-old woman with no prior history of uterine procedures. **(A)** Axial T2W MR image partially shows multiple subserosal leiomyomas *(f)* and a small hypointense nodule (arrow) along the right pelvic sidewall. **(B)** Axial T2W MR image at a slightly more inferior level shows a leiomyoma of the left broad ligament (∗), additional peritoneal nodules (arrows) in the cul-de-sac, and subserosal leiomyomas *(f)*. **(C)** Laparoscopic image of the right pelvic sidewall shows a fibroid uterus *(U)* medially and multiple nodules (arrows) along the right pelvic sidewall, one of which is seen in **A**.

Diffuse Peritoneal Leiomyomatosis

Diffuse peritoneal leiomyomatosis, also known as disseminated peritoneal leiomyomatosis, is a rare benign condition in which multiple firm nodules are scattered along the pelvic peritoneum (Fig 16) (10,74). These nodules are derived from the metaplasia of submesothelial cells and are histologically identical to typical or cellular leiomyoma, with little or no cytologic atypia and low mitotic activity. They are usually seen in high-estrogen settings, such as pregnancy and oral contraceptive use. Diffuse peritoneal leiomyomatosis usually has a benign course, with spontaneous regression after hormone use has stopped. In terms of imaging, leiomyomatosis is better evaluated with MRI, and the nodules have an appearance similar to that of leiomyomas. Unlike with metastatic disease, with diffuse peritoneal leiomyomatosis, there is no evidence of omental caking or ascites.

Management Options and Role of Imaging

Asymptomatic individuals are usually managed expectantly without treatment. For symptomatic patients, the location of the leiomyoma and the patient's desire to maintain fertility are important management considerations. Surgical management includes myomectomy performed by using hysteroscopic, laparoscopic, and open resection approaches, depending on the location and number of leiomyomas, and hysterectomy. Nonsurgical interventions include uterine fibroid embolization (UFE) and MRI-guided focused US surgery. Medical management includes hormonal therapy to decrease bleeding and leiomyoma size and anti-inflammatory medications to control pain.

Myomectomy

Myomectomy is an option for patients who would like to improve or preserve fertility. It can be performed by using a hysteroscopic or laparoscopic approach, or with laparotomy.

Hysteroscopy is a minimally invasive endoscopic approach in which the uterus is accessed through the vagina and cervix for resection of submucosal leiomyomas (FIGO stages 0–2) (75,76). Due to abutment of the endometrium by FIGO stage 3 leiomyomas, FIGO recommends hysteroscopy as the standard procedure for the differentiation of FIGO stage 3 versus FIGO stage 2 leiomyomas (16). FIGO stage 3 or 4 lesions are more often removed laparoscopically or with laparotomies (9). The *intramural extension,* defined as the shortest distance between the uterine serosa and deepest portion of the leiomyoma from the endometrium, should be measured (77). This is an important feature for determining the feasibility of hysteroscopic resection: If the distance is less than 5–8 mm, intraoperative US and/or laparoscopy may be needed to prevent uterine rupture or injury to extrauterine structures (78).

Laparoscopic and Open Hysterectomy

Symptomatic leiomyomas are one of the main indications for hysterectomy, which has long been considered the standard surgical treatment, particularly for patients who do not desire fertility preservation. Laparoscopic access is commonly used, but if the uterine volume is greater than or equal to the volume at 15–16 weeks pregnancy or the weight is more than 500 g, open hysterectomy is preferred owing to difficulty gaining laparoscopic access to the uterine vascular pedicles and suboptimal visualization of adjacent structures, which increase the risk of injury (79,80).

Uterine Fibroid Embolization

UFE is a nonsurgical complete uterine therapy performed by injecting embolizing material into the uterine arteries. Most leiomyomas can be targeted simultaneously, as they are generally supplied by the uterine arteries, resulting in infarction and shrinkage of leiomyomas while the myometrium revascularizes (76). The advantages of using UFE include a shorter recovery time, shorter hospital stay, and quicker return to daily function, as it is performed with use of local anesthesia.

Indications for UFE include bulk-related symptoms, menorrhagia, and anemia. Preprocedural MRI should be performed for evaluation of the presence of leiomyoma enhancement and potential ovarian artery supply to leiomyomas. Contraindications to UFE include pregnancy, uterine malignancy, and pelvic inflammatory disease. A subserosal

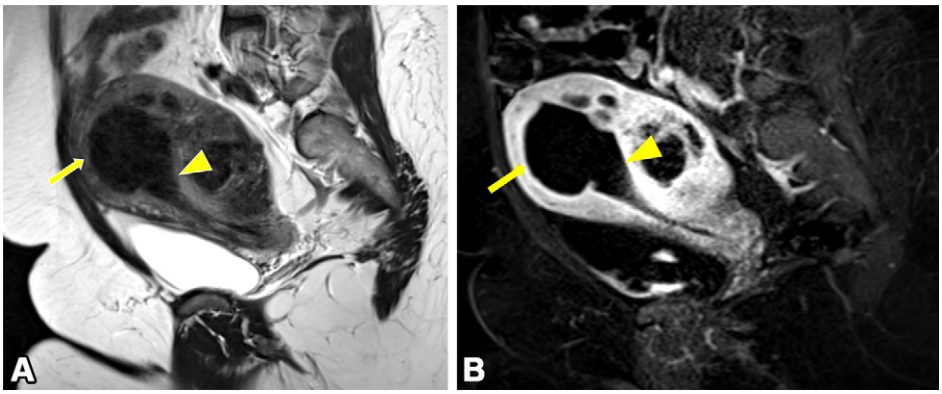

Figure 17. Numerous uterine fibroids treated with uterine fibroid embolization (UFE) in a 40-year-old woman with menorrhagia. Sagittal T2W **(A)** and post-contrast T1W fat-saturated subtraction **(B)** MR images after UFE show the leiomyoma (arrow), which decreased in size. The posterior aspect (arrowhead) of the leiomyoma has a triangular morphology, with the apex extending into the endometrial cavity, compatible with sloughing. The T1W image **(B)** shows no residual enhancement within the sloughing leiomyoma.

tumor location was once considered a relative contraindication owing to the risk of the leiomyoma sloughing into the peritoneal cavity; however, studies (81) have now shown no significant complications, and symptomatic improvement posttreatment. Leiomyomas with a submucosal component can slough off into the endometrial canal with expulsion or transvaginal sloughing (Fig 17). Imaging should be used to determine the interface-leiomyoma dimension ratio, as it may be helpful in predicting leiomyoma sloughing (82). Persistent early enhancement and a lack of size reduction after treatment may be due to insufficient embolization (potentially with an ovarian artery supply), but it also raises concern for the presence of an underlying sarcoma, and surgical removal should be considered.

MRI-guided High-Intensity Focused US

High-intensity focused US (HIFU) is MRI-guided, targeted, US-directed thermal ablation of a leiomyoma that results in tissue necrosis. Indications are similar to those for UFE, but patients with more than four leiomyomas or leiomyoma volumes greater than 500 mL are not considered optimal candidates for HIFU (83). Contraindications include leiomyoma factors such as pedunculated or calcified leiomyomas and patient factors such as pelvic malignancy or infection and pregnancy. Additional contraindications include inferior abdominal wall scarring and loops of bowel and adjacent sacral nerve roots in the treatment trajectory path, which can increase the risk of complications such as skin burn and intestinal perforation (84). Leiomyomas with high signal intensity on T2W MR images have high cellular contents that can be due to cellularity, edema, high vascularity, cystic degeneration, and/or myxoid degeneration resulting in resistance to energy or heat dissipation. Therefore, homogeneously T2-hyperintense leiomyomas are generally excluded from HIFU (85). After treatment, the nonperfused volume percentage of the leiomyoma is measured as an indicator of the level of treatment success (85).

Conclusion

Imaging evaluation of uterine leiomyoma has a key role in confirming the diagnosis and guiding management and is most accurately executed by using MRI. The location of the leiomyoma, together with the patient's desire to maintain fertility, drives management options for symptomatic leiomyomas. Localization with use of the FIGO classification system allows a consistent approach. Although conventional leiomyoma has a classic imaging appearance, radiologists need to be familiar with the subtypes, degeneration, and unusual growth patterns of these tumors, which can alter the imaging appearance. In postmenopausal patients, a new or enlarging uterine mass with solid enhancing intermediate or high signal intensity on T2W MR images and high signal intensity on high–*b*-value diffusion-weighted images, with corresponding low ADC signal intensity, is concerning for leiomyosarcoma.

Due to overlap of the imaging features of leiomyosarcoma with those of leiomyoma subtypes and degeneration, diagnostic algorithms, radiomics, and machine learning strategies are being developed in ongoing studies to optimize early imaging-based diagnoses. In these cases, gynecologic consultation with multidisciplinary discussion should be suggested for clinical risk stratification.

Author affiliations.—From the Department of Medical Imaging, University of Alberta, 116 St and 85 Ave, Edmonton, Alberta, Canada T6G 2R3 (W.T.); Department of Radiology (M.Y.) and Department of Laboratory Medicine and Pathology (L.C.), Mayo Clinic Arizona, Phoenix, AZ; Department of Radiology, University of Ottawa, Ottawa, Ontario, Canada (N.S.); Department of Medical Imaging, University Medical Imaging Toronto, University of Toronto, Toronto, Ontario, Canada (S.K.); and Department of Radiology, Brigham and Women's Hospital, Harvard University, Boston, MA (R.V.G., R.A.[1]). Presented as an education exhibit at the 2021 RSNA Annual Meeting. Received June 27, 2022; revision requested October 25 and received November 16; accepted November 18. **Address correspondence to** W.T. (email: *wendy.tu@ualberta.ca*).

Current address.—[1]**R.A.** Scientia Imaging, ScientiaImaging.com, Newton, MA.

Disclosures of conflicts of interest.—All authors have disclosed no relevant relationships.

References

1. Ross RK, Pike MC, Vessey MP, Bull D, Yeates D, Casagrande JT. Risk factors for uterine fibroids: reduced risk associated with oral contraceptives. Br Med J (Clin Res Ed) 1986;293(6543):359–362.
2. Mutter G, Prat J. Pathology of the Female Reproductive Tract. 3rd ed. Elsevier; 2014.
3. Baird DD, Dunson DB, Hill MC, Cousins D, Schectman JM. High cumulative incidence of uterine leiomyoma in black and white women: ultrasound evidence. Am J Obstet Gynecol 2003;188(1):100–107.
4. Marshall LM, Spiegelman D, Barbieri RL, et al. Variation in the incidence of uterine leiomyoma among premenopausal women by age and race. Obstet Gynecol 1997;90(6):967–973.
5. Kim JJ, Sefton EC. The role of progesterone signaling in the pathogenesis of uterine leiomyoma. Mol Cell Endocrinol 2012;358(2):223–231.

6. Wise LA, Palmer JR, Harlow BL, et al. Risk of uterine leiomyomata in relation to tobacco, alcohol and caffeine consumption in the Black women's health study. Hum Reprod 2004;19(8):1746–1754.
7. Baird DD, Dunson DB. Why is parity protective for uterine fibroids? Epidemiology 2003;14(2):247–250.
8. World Health Organization. WHO Classification of Tumours: Female Genital Tumours, 5th ed. International Agency for Research on Cancer Publications website. https://www.iarc.who.int/news-events/publication-of-the-who-classification-of-tumours-5th-edition-volume-4-female-genital-tumours/. Published September 9, 2020. Accessed July 5, 2022.
9. Munro MG, Critchley HOD, Fraser IS; FIGO Menstrual Disorders Committee. The two FIGO systems for normal and abnormal uterine bleeding symptoms and classification of causes of abnormal uterine bleeding in the reproductive years: 2018 revisions. Int J Gynaecol Obstet 2018;143(3):393–408. [Published correction appears in Int J Gynaecol Obstet 2019;144(2):237.]
10. Ueda H, Togashi K, Konishi I, et al. Unusual appearances of uterine leiomyomas: MR imaging findings and their histopathologic backgrounds. RadioGraphics 1999;19(Spec Issue):S131–S145.
11. Hricak H, Tscholakoff D, Heinrichs L, et al. Uterine leiomyomas: correlation of MR, histopathologic findings, and symptoms. Radiology 1986;158(2):385–391.
12. Mittl RL Jr, Yeh IT, Kressel HY. High-signal-intensity rim surrounding uterine leiomyomas on MR images: pathologic correlation. Radiology 1991;180(1):81–83.
13. Kubik-Huch RA, Weston M, Nougaret S, et al. European Society of Urogenital Radiology (ESUR) Guidelines: MR Imaging of Leiomyomas. Eur Radiol 2018;28(8):3125–3137.
14. Yamashita Y, Torashima M, Takahashi M, et al. Hyperintense uterine leiomyoma at T2-weighted MR imaging: differentiation with dynamic enhanced MR imaging and clinical implications. Radiology 1993;189(3):721–725.
15. Bakir B, Bakan S, Tunaci M, et al. Diffusion-weighted imaging of solid or predominantly solid gynaecological adnexial masses: is it useful in the differential diagnosis? Br J Radiol 2011;84(1003):600–611.
16. Munro MG, Critchley HO, Broder MS, Fraser IS; FIGO Working Group on Menstrual Disorders. FIGO classification system (PALM-COEIN) for causes of abnormal uterine bleeding in nongravid women of reproductive age. Int J Gynaecol Obstet 2011;113(1):3–13.
17. Laughlin-Tommaso SK, Hesley GK, Hopkins MR, Brandt KR, Zhu Y, Stewart EA. Clinical limitations of the International Federation of Gynecology and Obstetrics (FIGO) classification of uterine fibroids. Int J Gynaecol Obstet 2017;139(2):143–148.
18. Gomez E, Nguyen MT, Fursevich D, Macura K, Gupta A. MRI-based pictorial review of the FIGO classification system for uterine fibroids. Abdom Radiol (NY) 2021;46(5):2146–2155.
19. Zepiridis LI, Grimbizis GF, Tarlatzis BC. Infertility and uterine fibroids. Best Pract Res Clin Obstet Gynaecol 2016;34:66–73.
20. Madan R. The bridging vascular sign. Radiology 2006;238(1):371–372.
21. Tasaki A, Asatani MO, Umezu H, et al. Differential diagnosis of uterine smooth muscle tumors using diffusion-weighted imaging: correlations with the apparent diffusion coefficient and cell density. Abdom Imaging 2015;40(6):1742–1752.
22. Akbulut M, Gündoğan M, Yörükoğlu A. Clinical and pathological features of lipoleiomyoma of the uterine corpus: a review of 76 cases. Balkan Med J 2014;31(3):224–229.
23. Wang X, Kumar D, Seidman JD. Uterine lipoleiomyomas: a clinicopathologic study of 50 cases. Int J Gynecol Pathol 2006;25(3):239–242.
24. Bennett JA, Lamb C, Young RH. Apoplectic Leiomyomas: A Morphologic Analysis of 100 Cases Highlighting Unusual Features. Am J Surg Pathol 2016;40(4):563–568.
25. Persaud V, Arjoon PD. Uterine leiomyoma. Incidence of degenerative change and a correlation of associated symptoms. Obstet Gynecol 1970;35(3):432–436.
26. Nakai G, Yamada T, Hamada T, et al. Pathological findings of uterine tumors preoperatively diagnosed as red degeneration of leiomyoma by MRI. Abdom Radiol (NY) 2017;42(7):1825–1831.
27. Kawakami S, Togashi K, Konishi I, et al. Red degeneration of uterine leiomyoma: MR appearance. J Comput Assist Tomogr 1994;18(6):925–928.
28. Chesnais AL, Watkin E, Beurton D, Devouassoux-Shisheboran M. Myxoid mesenchymal tumors of uterus: endometrial stromal and smooth muscle tumors, myxoid variant [in French]. Ann Pathol 2011;31(3):152–158.
29. Bura V, Pintican RM, David RE, et al. MRI findings in-between leiomyoma and leiomyosarcoma: a Rad-Path correlation of degenerated leiomyomas and variants. Br J Radiol 2021;94(1125):20210283.
30. Arleo EK, Schwartz PE, Hui P, McCarthy S. Review of Leiomyoma Variants. AJR Am J Roentgenol 2015;205(4):912–921.
31. Jalaguier-Coudray A, Allain-Nicolai A, Thomassin-Piana J, et al. Radio-surgical and pathologic correlations of pelvic intravenous leiomyomatosis. Abdom Radiol (NY) 2017;42(12):2927–2932.
32. Yu X, Zhang G, Lang J, Liu B, Zhao D. Factors Associated With Recurrence After Surgical Resection in Women With Intravenous Leiomyomatosis. Obstet Gynecol 2016;128(5):1018–1024.
33. Gupta M, Laury AL, Nucci MR, Quade BJ. Predictors of adverse outcome in uterine smooth muscle tumours of uncertain malignant potential (STUMP): a clinicopathological analysis of 22 cases with a proposal for the inclusion of additional histological parameters. Histopathology 2018;73(2):284–298.
34. Lin G, Yang LY, Huang YT, et al. Comparison of the diagnostic accuracy of contrast-enhanced MRI and diffusion-weighted MRI in the differentiation between uterine leiomyosarcoma/smooth muscle tumor with uncertain malignant potential and benign leiomyoma. J Magn Reson Imaging 2016;43(2):333–342.
35. Cornfeld D, Israel G, Martel M, Weinreb J, Schwartz P, McCarthy S. MRI appearance of mesenchymal tumors of the uterus. Eur J Radiol 2010;74(1):241–249.
36. Fasih N, Prasad Shanbhogue AK, Macdonald DB, et al. Leiomyomas beyond the uterus: unusual locations, rare manifestations. RadioGraphics 2008;28(7):1931–1948.
37. Abramson S, Gilkeson RC, Goldstein JD, Woodard PK, Eisenberg R, Abramson N. Benign metastasizing leiomyoma: clinical, imaging, and pathologic correlation. AJR Am J Roentgenol 2001;176(6):1409–1413.
38. Arai T, Yasuda Y, Takaya T, Shibayama M. Natural decrease of benign metastasizing leiomyoma. Chest 2000;117(3):921–922.
39. Seagle BL, Sobecki-Rausch J, Strohl AE, Shilpi A, Grace A, Shahabi S. Prognosis and treatment of uterine leiomyosarcoma: a National Cancer Database study. Gynecol Oncol 2017;145(1):61–70.
40. Hartmann KE, Fonnesbeck C, Surawicz T, et al. Management of Uterine Fibroids: Comparative Effectiveness Review, No. 195. Agency for Healthcare Research and Quality website. https://www.ncbi.nlm.nih.gov/books/NBK537742/. Published December 2017. Accessed July 5, 2022.
41. Roberts ME, Aynardi JT, Chu CS. Uterine leiomyosarcoma: a review of the literature and update on management options. Gynecol Oncol 2018;151(3):562–572.
42. Hosh M, Antar S, Nazzal A, Warda M, Gibreel A, Refky B. Uterine Sarcoma: Analysis of 13 089 Cases Based on Surveillance, Epidemiology, and End Results Database. Int J Gynecol Cancer 2016;26(6):1098–1104.
43. Brooks SE, Zhan M, Cote T, Baquet CR. Surveillance, epidemiology, and end results analysis of 2677 cases of uterine sarcoma 1989-1999. Gynecol Oncol 2004;93(1):204–208.
44. Sala E, Rockall AG, Freeman SJ, Mitchell DG, Reinhold C. The added role of MR imaging in treatment stratification of patients with gynecologic malignancies: what the radiologist needs to know. Radiology 2013;266(3):717–740.
45. Thomassin-Naggara I, Dechoux S, Bonneau C, et al. How to differentiate benign from malignant myometrial tumours using MR imaging. Eur Radiol 2013;23(8):2306–2314.
46. Giuntoli RL 2nd, Metzinger DS, DiMarco CS, et al. Retrospective review of 208 patients with leiomyosarcoma of the uterus: prognostic indicators, surgical management, and adjuvant therapy. Gynecol Oncol 2003;89(3):460–469.
47. Żak K, Zaremba B, Rajtak A, Kotarski J, Amant F, Bobiński M. Preoperative Differentiation of Uterine Leiomyomas and Leiomyosarcomas: Current Possibilities and Future Directions. Cancers (Basel) 2022;14(8):1966.
48. Goto A, Takeuchi S, Sugimura K, Maruo T. Usefulness of Gd-DTPA contrast-enhanced dynamic MRI and serum determination of LDH and its isozymes in the differential diagnosis of leiomyosarcoma from degenerated leiomyoma of the uterus. Int J Gynecol Cancer 2002;12(4):354–361.
49. Bast RC Jr, Klug TL, St John E, et al. A radioimmunoassay using a monoclonal antibody to monitor the course of epithelial ovarian cancer. N Engl J Med 1983;309(15):883–887.
50. American College of Obstetricians and Gynecologists' Committee on Gynecologic Practice. Uterine Morcellation for Presumed Leiomyomas: ACOG Committee Opinion, Number 822. Obstet Gynecol 2021;137(3):e63–e74. [Published correction appears in Obstet Gynecol 2021;138(2):313.]
51. Product Labeling for Laparoscopic Power Morcellators. U.S. Food and Drug Administration website. https://www.fda.gov/regulatory-information/search-fda-guidance-documents/product-labeling-laparoscopic-power-morcellators. Published 2020. Accessed July 5, 2022.
52. Grady D. Amy Reed, Doctor Who Fought a Risky Medical Procedure, Dies at 44. The New York Times website. https://www.nytimes.com/2017/05/24/us/amy-reed-died-cancer-patient-who-fought-morcellation-procedure.html. Published May 24, 2017. Accessed July 5, 2022.
53. Multinu F, Casarin J, Hanson KT, et al. Practice Patterns and Complications of Benign Hysterectomy Following the FDA Statement Warning Against the Use of Power Morcellation. JAMA Surg 2018;153(6):e180141.

54. Wright JD, Chen L, Burke WM, et al. Trends in Use and Outcomes of Women Undergoing Hysterectomy With Electric Power Morcellation. JAMA 2016;316(8):877–878.
55. FDA In Brief: FDA Takes Additional Actions to Increase the Safety of Laparoscopic Power Morcellators Used in Gynecologic Surgeries. U.S. Food and Drug Administration website. https://www.fda.gov/news-events/fda-brief/fda-brief-fda-takes-additional-actions-increase-safety-laparoscopic-power-morcellators-used. Published December 29, 2020. Accessed July 5, 2022.
56. Aviram R, Ochshorn Y, Markovitch O, et al. Uterine sarcomas versus leiomyomas: gray-scale and Doppler sonographic findings. J Clin Ultrasound 2005;33(1):10–13.
57. Sahdev A, Sohaib SA, Jacobs I, Shepherd JH, Oram DH, Reznek RH. MR imaging of uterine sarcomas. AJR Am J Roentgenol 2001;177(6):1307–1311.
58. Rio G, Lima M, Gil R, Horta M, Cunha TM. T2 hyperintense myometrial tumors: can MRI features differentiate leiomyomas from leiomyosarcomas? Abdom Radiol (NY) 2019;44(10):3388–3397.
59. Tanaka YO, Nishida M, Tsunoda H, Okamoto Y, Yoshikawa H. Smooth muscle tumors of uncertain malignant potential and leiomyosarcomas of the uterus: MR findings. J Magn Reson Imaging 2004;20(6):998–1007.
60. Kaganov H, Ades A, Fraser DS. Preoperative Magnetic Resonance Imaging Diagnostic Features of Uterine Leiomyosarcomas: A Systematic Review. Int J Technol Assess Health Care 2018;34(2):172–179.
61. Jagannathan JP, Steiner A, Bay C, et al. Differentiating leiomyosarcoma from leiomyoma: in support of an MR imaging predictive scoring system. Abdom Radiol (NY) 2021;46(10):4927–4935.
62. Shinya T, Shibamoto K, Maeba K, et al. Magnetic resonance imaging findings of a myxoid leiomyosarcoma of the uterus: a case report and literature review. Eur J Radiol Open 2021;8:100328.
63. Tamai K, Koyama T, Saga T, et al. The utility of diffusion-weighted MR imaging for differentiating uterine sarcomas from benign leiomyomas. Eur Radiol 2008;18(4):723–730.
64. Sato K, Yuasa N, Fujita M, Fukushima Y. Clinical application of diffusion-weighted imaging for preoperative differentiation between uterine leiomyoma and leiomyosarcoma. Am J Obstet Gynecol 2014;210(4):368.e1–368.e8, e8.
65. Namimoto T, Yamashita Y, Awai K, et al. Combined use of T2-weighted and diffusion-weighted 3-T MR imaging for differentiating uterine sarcomas from benign leiomyomas. Eur Radiol 2009;19(11):2756–2764.
66. Hindman N, Kang S, Fournier L, et al. MRI Evaluation of Uterine Masses for Risk of Leiomyosarcoma: A Consensus Statement. Radiology 2023;306(2):1–15.
67. Abdel Wahab C, Jannot AS, Bonaffini PA, et al. Diagnostic Algorithm to Differentiate Benign Atypical Leiomyomas from Malignant Uterine Sarcomas with Diffusion-weighted MRI. Radiology 2020;297(3):E347.
68. Lakhman Y, Veeraraghavan H, Chaim J, et al. Differentiation of Uterine Leiomyosarcoma from Atypical Leiomyoma: Diagnostic Accuracy of Qualitative MR Imaging Features and Feasibility of Texture Analysis. Eur Radiol 2017;27(7):2903–2915.
69. Nakagawa M, Nakaura T, Namimoto T, et al. A multiparametric MRI-based machine learning to distinguish between uterine sarcoma and benign leiomyoma: comparison with ^{18}F-FDG PET/CT. Clin Radiol 2019;74(2):167.e1–167.e7, e7.
70. Rockall AG, Sohaib SA, Harisinghani MG, et al. Diagnostic performance of nanoparticle-enhanced magnetic resonance imaging in the diagnosis of lymph node metastases in patients with endometrial and cervical cancer. J Clin Oncol 2005;23(12):2813–2821.
71. Malek M, Tabibian E, Rahimi Dehgolan M, et al. A Diagnostic Algorithm using Multi-parametric MRI to Differentiate Benign from Malignant Myometrial Tumors: Machine-Learning Method. Sci Rep 2020;10(1):7404.
72. Leren V, Langebrekke A, Qvigstad E. Parasitic leiomyomas after laparoscopic surgery with morcellation. Acta Obstet Gynecol Scand 2012;91(10):1233–1236.
73. Lu B, Xu J, Pan Z. Iatrogenic parasitic leiomyoma and leiomyomatosis peritonealis disseminata following uterine morcellation. J Obstet Gynaecol Res 2016;42(8):990–999.
74. Levy AD, Arnáiz J, Shaw JC, Sobin LH. From the archives of the AFIP: primary peritoneal tumors—imaging features with pathologic correlation. RadioGraphics 2008;28(2):583–607; quiz 621–622.
75. Baumgarten MN, Polanski LT. Modern management of fibroids. Obstet Gynaecol Reprod Med 2020;30(4):104–108.
76. Donnez J, Dolmans MM. Uterine fibroid management: from the present to the future. Hum Reprod Update 2016;22(6):665–686.
77. Wamsteker K, Emanuel MH, de Kruif JH. Transcervical hysteroscopic resection of submucous fibroids for abnormal uterine bleeding: results regarding the degree of intramural extension. Obstet Gynecol 1993;82(5):736–740.
78. Leone FP, Lanzani C, Ferrazzi E. Use of strict sonohysterographic methods for preoperative assessment of submucous myomas. Fertil Steril 2003;79(4):998–1002.
79. Donnez O, Donnez J. A series of 400 laparoscopic hysterectomies for benign disease: a single centre, single surgeon prospective study of complications confirming previous retrospective study. BJOG 2010;117(6):752–755.
80. Sinha R, Sundaram M, Lakhotia S, Mahajan C, Manaktala G, Shah P. Total laparoscopic hysterectomy for large uterus. J Gynecol Endosc Surg 2009;1(1):34–39.
81. Silberzweig JE, Powell DK, Matsumoto AH, Spies JB. Management of Uterine Fibroids: A Focus on Uterine-sparing Interventional Techniques. Radiology 2016;280(3):675–692.
82. Verma SK, Bergin D, Gonsalves CF, Mitchell DG, Lev-Toaff AS, Parker L. Submucosal fibroids becoming endocavitary following uterine artery embolization: risk assessment by MRI. AJR Am J Roentgenol 2008;190(5):1220–1226.
83. Roberts A. Magnetic resonance-guided focused ultrasound for uterine fibroids. Semin Intervent Radiol 2008;25(4):394–405.
84. Arleo EK, Khilnani NM, Ng A, Min RJ. Features influencing patient selection for fibroid treatment with magnetic resonance-guided focused ultrasound. J Vasc Interv Radiol 2007;18(5):681–685.
85. Machtinger R, Inbar Y, Cohen-Eylon S, Admon D, Alagem-Mizrachi A, Rabinovici J. MR-guided focus ultrasound (MRgFUS) for symptomatic uterine fibroids: predictors of treatment success. Hum Reprod 2012;27(12):3425–3431.